Anonymous Referee #RC1

Referee comments on "A new method for operating a continuous flow diffusion chamber to investigate immersion freezing: assessment and performance study" by Gourihar Kulkarni, Naruki Hiranuma, Ottmar Möhler, Kristina Höhler, Swarup China, Daniel J. Cziczo and Paul J. DeMott

Overview:

This paper is a useful addition to the literature on INP measurements in general and to the many reported uses of CFDC instruments in particular. A new mode of operation for a CFDC-type instruments is proposed and evaluated in the paper. In this mode, immersion freezing measurements over a range of temperatures are obtained with steady cooling rather than in the more customary mode of single temperature or step-wise cooling. What is called the evaporation section for many CFDC instruments is changed to nucleation section in this paper.

The proposed method puts emphasis on the temperature dependence of INP activity whereas much of the CFDF literature deals with the dependence of nucleation on humidity, although there is a large range of types and operating modes of CFDC instruments (cf. Hiranuma et al. 2015, with Supplement). The question of the relative importance in these chambers of activation via deposition or freezing is sidestepped in the current paper. It is also set aside in these comments because of the general view that immersion freezing is dominant in most cases.

From an operational point of view, the evaporation of the drops at the low RHw of the nucleation section avoids the possibility of droplets being counted at the outlet. This avoids one of the common problems with CFDC instruments.

The authors have done a number of tests to support the results presented and examined some potential error sources. However, probably because the approach is new, additional questions arise and some aspects of the measurement method require further scrutiny.

Reply: Thanks for the reviews and feedback.

Exposure time and temperature:

This issue can be addressed principally on the basis of the simulations presented in Section 2.2 of the paper and in the Appendix. According to these calculations droplets rapidly decrease in size at the same time as the

temperature adjusts to the temperature of the nucleation chamber, Tnc. The minimum droplet sizes shown occur when the temperature is within about 1 C of Tnc. Furthermore, the comparison in Fig. S5 shows that variations in the entry position of the aerosol do not add further errors. From these results it would follow that all droplets reach the set temperature of the nucleation sections within errors comparable to other instrumental uncertainties.

However, the simulations are for ideal laminar flow. **To what extent is this actually the case? How much extra spread is caused by deviations from the ideal flow and by polydisperse INP sizes?** Larger drops might evaporate later but the temperature they reach would not differ from the set value. But, if there are droplets that evaporate faster than the simulated values, these would have a higher minimum temperature of exposure and that would lead to underestimates of the final results. Since Fig. 7 shows that derived ns values are higher than those reported in other papers for three out of the four samples tested, it appears that there is no major problem in this regard.

Reply: Agree, these simulations are for ideal laminar flow. To quantify the particles outside of the lamina, pulse test experiments using monodisperse particles are performed. These results are presented in Figure S1 in the original manuscript.

The following text and figure are added to the revised manuscript.

Section 2.1: *Simulations (see below) are performed to investigate the sensitivity of polydisperse particles. The particle residence time of three different monodisperse particles (0.3 μm, 1.0 μm, and 2.0 μm) traversing the chamber is calculated. Results show that the residence time of these particles is similar indicating monodisperse size pulse experiments are also applicable to other size particles.*
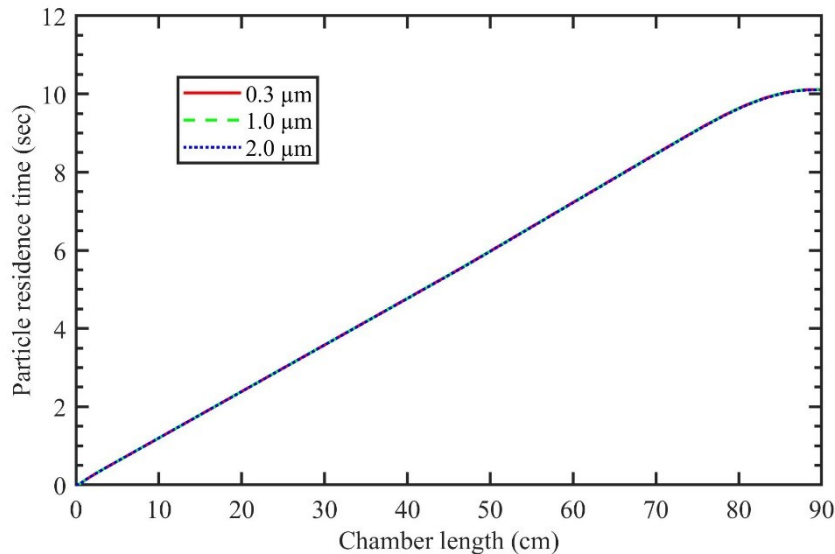
Figure S1: Particle residence time of different size droplets within the chamber.

60 More importantly, the short exposure time of INPs to the coldest temperature necessitates consideration of the time dependence of nucleation. Cooling rates of the droplets when entering the nucleation section approach 10°C sec^{-1} for the lowest Tnc value. For such rapid cooling, Eq. 5 from Vali and Snider (2015) with ξ = 0.3 indicates a 2°C shift toward colder temperatures compared to a 1°C min^{-1} rate of cooling, i.e. the same activity would be observed with 2°C additional cooling[1]. With that correction, **the current data in Fig. 7 would have to be represented by**
65 **points shifted to the right** to bring the comparison on the same basis as the other data, although the exact cooling rates associated with each data set from the literature would have to be considered as well.

The tests with constant temperature of the nucleation section (lines 274-281 and solid squares in Fig. 6) do not address the point raised above. This is because the 0.5° C min^{-1}cooling rate is negligible compared to the rapid cooling of the drops on transition from the conditioning to the nucleation section.

70 While there is no a priori reason for assuming that activity has to rise exponentially, it is also worth considering **whether rapid cooling in these experiments may explain why** the slopes of the ns versus T data points in Fig 7 flatten out at colder temperatures. As can be seen from the Figs. S2 to S5, the lower Tnc is, the faster the cooling is and thus **larger corrections (moving points to higher temperatures) would be necessary to normalize the data** to a fixed cooling rate.

75 [1]There is no empirical evidence to support the use of the equation for cooling rates 600 times over the reference value, but there is no other basis at this time to make a better estimate.

From the above it follows that the rapid cooling occurring in the transition from the conditioning section to the nucleation section **influences** both the magnitudes of the derived ns values and the slopes of the temperature spectra. **The authors' view of this would make the paper more complete**.

80 **Reply**: We appreciate these comments. Previously, time-dependent immersion freezing framework (e.g. Vali and Snider (2015), Herbert et al. (2014)) had been formulated to understand time dependent nature of ice nucleation. The framework allows to correct the shift in temperature towards colder temperature for a given change in cooling rate. The cooling rate constant ξ depends on the nature of the INP population, and this constant varies from ~0.15 to 1.6 (Table 2, Herbert et al. (2014)). In this work, we investigated various test species (K-feldspar,
85 airborne soil dusts from the arable region, illite-NX, and Argentinian soil dust), and the ξ values for each of these species for the droplet conditions (size and one INP per droplet) that are used in this work are unknown. Therefore, the application of such an empirical relationship to correct for the shift in temperature because of the droplet cooling rate is not possible currently. These parameters can be obtained by conducting immersion freezing tests using direct processing (e.g. CFDC style instruments) and post-processing (e.g. BINARY style
90 instrument) in parallel.

It should be noted that our experiments shown as solid squares in Fig. 6 do indicate the minimal influence of rapid cooling on ice fraction or n_s values. In this experiment, the nucleation section is held constant at one temperature, and while the droplets are transitioning from the conditioning section to the nucleation section, the droplets undergo rapid cooling. Please see the discussion in section 3.

95 We added the following paragraph to acknowledge the possibility of influence on reported temperatures because of rapid cooling.

Section 3: *Further, the time-dependent immersion freezing framework (e.g. Vali and Snider (2015), Herbert et al. (2014)) suggests that the rapid cooling of the droplets could shift the cumulative ice fraction towards the colder temperature based on the cooling rate and particular INP material constant. However, these input parameters for the time-dependent model are not available currently to quantify the temperature shift for the present experimental conditions. Future studies that involves collocated direct and post-processing INP instruments would be needed.*

Sensitivity and error analysis:

The paper states that it is possible to execute three test cycles before icing problems. It also states (line 256) that full temperature spectra were acquired in about 30 minutes. However, information about the **input aerosol concentrations** used in the tests wasn't readily found in the paper. The temperatures of the tests for the airborne dust were restricted to -28°C and colder. It would be useful **to know more about sample concentration** (in terms of active number at test temperatures), and **sampling duration requirements versus statistical counting errors**. Perhaps this sort of analysis formed the basis for the accuracy estimates indicated on lines 263-265 of the paper but it is unclear if that is the case.

Reply: We added the following sentence.

Section 2.4: *The input aerosol concentration of all four INP species varied from 100 to 800 # per cubic centimeters, and the sampling duration was ~30 minutes.*

The statistical counting error is considered by calculating the standard deviation of the ice fraction measurements. This is discussed in the original manuscript on line 247.

Minor points:

line 21 and other places: Is arable dust a soil science definition? Perhaps the meaning of the term could be clarified for the context used here. Desert dust? Top soil? Agricultural dust? A detailed description of the sample is given on lines 240 on but the term is used already in the abstract and is frequently used in the paper prior to the definition.

Reply: We modified the definition. The revised definition (in bold) reads as follows.

Abstract: *The performance of the MCIC was evaluated using four INP species: K-feldspar, illite-NX, Argentinian soil dust, and **airborne soil dusts from an arable region** that had shown ice nucleation over a wide span of supercooled temperatures.*

Abstract: *… during the second phase of the Fifth International Ice Nucleation Workshop (FIN-02) campaign, and **airborne arable soil dust** particles were sampled…*

Section 2.4: The arable soil dust is defined as follows.

***Airborne soil dust from the arable region** or shortly airborne arable dust particles* were sampled at the PNNL sampling site during a regional windblown dust event.

line 62: "sequence' might be better here than "spectrum".

Reply: Corrected.

line 164: The point about not simulating nucleation is mentioned because of the possible latent heat effect or some other argument?

Reply: CFD simulations described in section 2.2 do not involve droplet freezing (or nucleation of ice) simulations. This is not performed because the objective of numerical simulations was to better understand the flow behavior and their impact on droplet dynamics (growth and evaporation). The following sentence added to section 2.2 clarifies the goal of this section.

Section 2.2: *At the entrance of the nucleation section, the temperature and RHw profiles can be unsteady, and to better understand the flow patterns of these profiles within the transitioning zone, and its impact on droplet behavior, numerical simulations using computational fluid dynamics (CFD) are performed.*

line 290: The approximation indicated is valid only for Fice << 1:0

Reply: Correct. This assumption of approximation is mentioned in the main text.

Section 3: *The approximation is valid for ice fraction << 1.0.*

170

Anonymous Referee #RC2
Referee comments on "A new method for operating a continuous flow diffusion chamber
to investigate immersion freezing: assessment and performance study" by G. Kulkarni
et al. 2020

175

In the submitted manuscript Kulkarni et al. describe a new method for operating a Continuous Flow
Diffusion Chamber (CFDC) and show both system modeling results and results from testing using
various experimental test aerosol and some ambient air sampling. I find the manuscript generally
well written and presented. The idea for the new CFDC operation principle is original and enticing.
180   This idea potentially expands the operational range of CFDC instruments and could be a significant
contribution to the community. However in its current form the submitted work lacks clarity in some
key areas. Some additional work also needs to be done with respect to the figures, where either
interpretation is difficult and/or mistakes appear to have been made with labeling in the main text etc

Nucleation Temperature and Crystal Growth: I think the primary question that the authors must
185   clarify is related to quantifying the ice nucleation temperature and ice crystal growth within the evaporation (now
nucleation) section of the CFDC. The authors have done a nice job of trying to model
the droplet growth in the 'conditioning' section, but have **not shown analogous results for modeling
the crystal changes in the evaporation section** (I recognize they posit that given the saturation condition is RH$_{ice}$
= 100% there are no changes – but consider comment below). My interpretation of
190   Figure 4 and many of the Supplemental figures is that if the system behaves as modeled then liquid
droplets quickly evaporate within the nucleation section – on approximately the same time scale as
the temperature and RH fields equilibrate. This suggests that the nucleation occurs in this transition
region and that the fixed nucleation section temperature in fact controls the gradient between the two
sections **but does not necessarily represent the actual nucleation condition**. **What size water droplet
195   must nucleate into ice in order to grow to reach the quoted 3 _m OPC cutoff for ice?** If there is
a lower bound on this value then one might interpret before **what point along the droplet evaporation
curves ice must form**. Likewise it would be interesting to **understand the range of potential ice
crystal sizes** depending on at what point entering the chamber a droplet nucleates. Clearly at the
warmest temperatures the gradients between the two chambers are weaker and thus the constraints
200   on thermodynamic forcing will be better, but at the colder **temperatures I remain to convinced that the
nucleation occurs at the equilibrated chamber conditions.**

Reply: The evaporation section conditions are constant. This section is maintained at constant temperature and RH$_{ice}$ (=100%) conditions (Fig. 4a). We expect no change in the ice crystal size.

205 Correct, the temperature within the transition section (varies from conditioning section to nucleation or evaporation section) does not correspond to the equilibrium nucleation section temperature (e.g. Fig. S5 b). Freezing occurs at various temperatures that range from the conditioning section temperature (~ -20 °C) to the nucleation section temperature (e.g. -30°C) conditions. The temperature uncertainty across the aerosol lamina and nucleation section are ± 0.9 and ± 0.4°C, respectively. Here, we have used temperature uncertainty across

210 the nucleation section as the temperature uncertainty within the ice fraction. The ice fraction is defined as the cumulative fraction of the droplet frozen, and it is reported at the coldest section of the chamber (i.e. steady state nucleation section temperature). See supplementary section Text S1. Following sentence is added.

Text S1: *The freezing temperature (T) is defined at the steady state temperature of the nucleation section, and the*
215 *freezing temperature uncertainty is assumed to be similar to the uncertainty across the nucleation section (±*
0.4°C).

CFD simulations (e.g. Fig S3 c) show that water droplets of size greater than 2 µm in radius will mostly contribute towards nucleation of ice. Droplets smaller than this size are exposed to subsaturation conditions, and they
220 evaporate quickly (< 1 sec; see Fig S3 b). It should be noted that as nucleation occurs in the order of a few ms (Holden et al. 2019), the droplets smaller than 2 µm might also contribute towards nucleation of ice. However, the contribution of these smaller droplets of less than 2 µm is very small (see Fig. 5a).

Holden, M. A., Whale, T. F., Tarn, M. D., O'Sullivan, D., Walshaw, R. D., Murray, B. J., Meldrum, F. C., and
225 *Christenson, H. K.: High-speed imaging of ice nucleation in water proves the existence of active sites, Sci. Adv.,*
5, eaav4316, https://doi.org/10.1126/sciadv.aav4316*, 2019.*

Further evidence already included: on page 6 the authors state that, "ice particle size measured by the OPC can be representative of the size of the droplet while freezing." However, all simulations of
230 droplet growth suggest maximum droplet sizes between 2 and 2.5 _m. Figure 5 shows peak OPC concentrations from about 3.57 to 5.02 (diameter) which more-or-less corresponds to the peak predicted particle sizes, and those droplet diameters only occur immediately in this transition region and **not within the equilibrated portion of the chamber**. However, also to consider is that, although the equilibrated chamber represents RH$_{ice}$ = 100%, as long as **droplets do exist ice particles can grow**
235 **due to scavenging...to what extent? Perhaps this is minimal? Will the droplet evaporation go back to the walls?**
Reply: Figure 5a shows ice crystal sizes and their respective concentrations at different temperatures. As mentioned above, droplets of size less than 2 µm in radius may contribute towards the total ice crystal concentration, but their fraction compared to the total concentration is very small.
240

Flow conditions across the chamber are laminar (Fig. 4a). The droplets and ice crystals follow particle trajectories determined by the various forces (flow conditions and gravity) acting on the particle. It appears that these particles have insufficient inertia to cross the gas streamlines (Fig. S5; see five INP trajectories), such that scavenging of droplets by ice crystals can be ignored. Correct, the water vapor from the droplet (during
245 evaporation) might go towards the wall. Also, some of the vapor might exit the chamber.

Below I present an itemized list of additional thoughts and comments as I came to them in the text, which I hope helps to further contextualize my thoughts.

Itemized Scientific and Editorial Suggestions:

250 Specific Suggestions by Page and Line Number (page, line):
_ (1,26) enough to say sampled from 'am ambient aerosol inlet'. The location etc. is described later.
_ (2,42) replace toward with for
_ (2,50) percent
255 _ (2,50) CFDCs also
_ (2, 61) particles are activated not 'all aerosol'. Remember the strict definition of aerosol is the gas, particle mixture thus activation of all aerosol seems strange.
_ (3, 68) the Compact Ice...
Reply: All the above comments are addressed.

260 _ (3, 70) thermally isolated or insulated? How much thermal contact do the 2 sections actually have? **Reply**: Corrected, they are thermally isolated. The two walls are not in contact with each other, but they are separated by double-layered insulated gasket.

_ (3,78) Here begins the use of many symbols _, =_, etc. which continues throughout the manuscript
265 in an ill-defined manner. I presume most often these are being used to indicate approximately, for which I suggest _. Although definitions are a bit muddled the use of similar to _ to many, including me, denotes an order of magnitude (-ish) approximation. I am sure the authors intention is to convey a more approximate value than that in many of their uses here and throughout.
Reply: Corrected. The ~ symbol is replaced with ≈ symbol.
270
Here also the RHw is indicated as 106%. Later in the numerical modeling section 2.2 a RHw of 113% is chosen and this value also seems to be chosen in the experimental descriptions that follow. I am left confused, why these differences?
Reply: The RHw = 106% corresponds to the CIC chamber (the original chamber, but not the modified chamber or
275 MCIC). The RHw = 113% corresponds to the modified CIC chamber (MCIC).

_ (3, 80) An OPC
Reply: Corrected.

280 _ (3,93) Please also include here the saturation condition that results from the choice of temperatures – it would be nice to also have the value in terms of ice saturation.
Reply: The saturation (water and ice) conditions for these conditions are shown in Figure 3. We added the following sentence to address this comment.

285 Section 2.1: *The resulting water and ice saturation conditions are shown in Figure 3.*

_ (4, 103) 'The choice of steady-state cooling....' I think the manuscript would benefit from a longer

8

discussion related to the cooling rate. The empirical choice of cooling rate as being satisfactory is supported by the filled symbols on Figure 6, which I understand were measurements made with the

290 chamber at static conditions. However, did the authors try any other cooling rates? Do they have any evidence of what a maximum cooling rate might be? I think any additional information that might have been gathered with regard to the operational limits would add value to what the authors have done.

Reply: Some exploratory work with different cooling rates is explored. The ice fraction results of ambient sampling showed a negligible difference between the cooling rates.
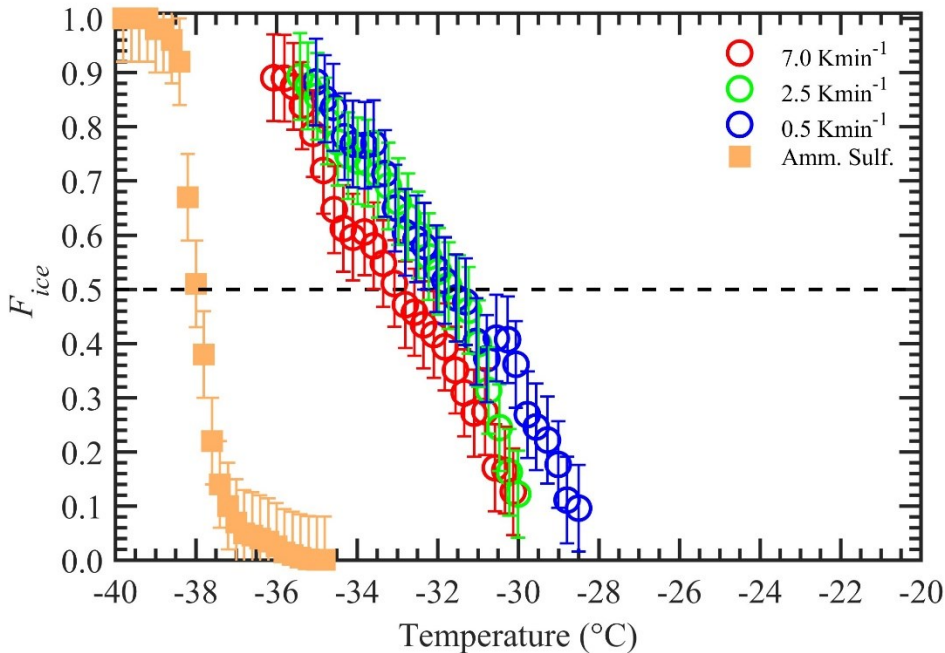
295

Figure S8: The F_{ice} of airborne arable dust species as a function of temperature and nucleation section cooling rates. The cooling rate of 0.5 Kmin^{-1} was used in this study.

300

The figure is added to the supplementary section. The following text is added to the manuscript.

Section 2.1: *The implications of higher cooling rates towards INP measurements were also explored.*
Section 3.0: *The experiments with higher cooling rates (2.5 and 7.0 °C min^{-1}) had also a negligible effect on F_{ice} of*

305 airborne arable dust species *(Figure S8).*

_ (4,110-113) More clarity is needed with respect to the pulse experiments. The pulse duration is quoted as 10.5 s. In Fig. 1 of the supplement the dashed line is used to indicate the limit after which particles are considered to be outside of the lamina. However, if the pulse duration is 10.5 s and

310 the residence time is _ 10s shouldn't pulsed particles continue to arrive until 20.5 s? This would presumably significantly alter the 16% number in the text. How is my understanding deficient?

9

Reply: The data is shown when CPC starts recording the particle counts. The below sentence is added to the figure caption of figure S1.

Figure S1*: The data is shown only when CPC started recording the particle counts.*

_ (4,113-116) Final sentence of this section seems to be better suited to introduce the following section.
Reply: Corrected.

_ (5,133-134) such a geometry; I am confused by the end to this sentence. "...it was coupled with energy and viscous heating to enable the species..." I think this needs to be reworded. What was coupled exactly? Is energy conservation meant? Please clarify this sentence.
Reply: Corrected. These sentences describe the viscous model used to model the flow and droplet trajectories. The sentence is revised as follows.

Section 2.2: *The viscous model – the standard RNG $\kappa - \varepsilon$ turbulence model was used. This model treats velocity fluctuations better than other turbulence models for such a geometry. This turbulence model was used in conjunction with species transport modeling capability such that the effects of smaller eddies of fluid motion are better captured.*

_ (5,141) I found the relevant information is S.1 not S1, but this appears very far into the supplement. It would be useful to order the supplement in an order that corresponds to how it is referenced in the text.
Reply: Sorry for the inconvenience. It should read S.1. To avoid the confusion, we rename it as Text S1.

The order of Text S1 and S2 is rearranged.

More notes with regard to S.1: What is meant with e_1 and e_r? The use of 'environment' is confusing. I think e_1 represents the far field vapor pressure, while e_r represents the equilibrium vapor pressure at the surface. Similarly the temperature terms should be precisely defined. Furthermore, the D_v term introduces another temperature T and pressure p that seem to have the same definitions as T_1 and e_1. Please use uniform notation and be clear.
Reply: Corrected.

Finally r_0 is the initial radius of the droplet, but by my reading, for the purposes of this manuscript r_0 has been set to equal the dry aerosol particle diameter. However, we know that at deliquescence (DRH) any soluble aerosol particle will have a sharp transition terms of growth factor (GF). For example at DRH the GF for NaCl jumps suddenly from 1 to _ $1:6_1$. How is this discontinuity accounted for? Even for mineral surfaces one would expect the r_0 to be potentially, importantly different when it is completely coated in bulk water versus when it is dry or just has adsorbed water present.
Reply: The r_0 sizes are already CCN sizes. We repeat the sentence already described in section 2.2.

10

355 The potential INPs are assumed (i.e., sub-saturated particle growth is ignored) to activate to droplets because they are greater than cloud condensation nuclei sizes (Seinfeld and Pandis, 2016) and grow as long as RHw is increasing or remains constant.

_ (5,143) Figure 2 is referred to but I believe the intent is Figure 4a perhaps?
Reply: Thanks. Yes, it is Figure 4a. The typo is corrected.

360

_ (5, 154) Figure S2-5: I found myself spending a lot of time digesting these figures and wonder if the authors should revisit what in fact **is best to include in the main text**. Perhaps they **might hybridize some current figures to add some detail to the main text** that only appears now in the supplement.
Reply: An example is already included in the main text. See Figure 4b. A reference to other supplementary figures
365 is included in the figure caption

I would also suggest that in Figures S2-S4 the authors choose different color maps for time and RH.
Reply: Thanks for the suggestion. This is tried but gets overly complicated to interpret the results. The choice of similar colormap is justified because then it is easy to compare the low and high values using consistent colors.

370

With 2 color maps and an offset perhaps panels b and c could potentially be combined. Even if not flipping between figures would be easier if the color maps differed.
Reply: Addressed above.

375 Figure S5 is missing a legend. Also in this figure the red droplet radius points seem problematic. Firstly, they seem to show a discontinuity at the chamber transition that none of the other curves indicate.

Second, one would intuitively expect their values to perhaps lie between the black and pink, but also the red temperature seems to be lower than the black as it gets close to the transition. Why does the particle further
380 from the cold wall have a colder temperature than that which is closer? I find that a clear explanation of this figure, and especially the reason the red points stand out is lacking.
Reply: The legend is like in Figure S4. The following sentence is added to the caption.

Figure S5: *The plotted data line style and marker symbol are similar to the legend described in Figure S4.*

385

_ (6, 167) Table S1: replace very small with _ X.
Reply: Corrected.

_ (6, 169) evaporating droplet
390 **Reply**: Corrected.

_ (6, 175) 200 nm? Why not use 300 nm to match the simulations? Perhaps a comment on this choice would be useful.
Reply: The choice was based on the optimization of two factors: number concentration and monodisperse size.
395 This size allowed us to generate the maximum number of monodisperse particles. Generating smaller sizes

11

produces multiple charge particles, whereas generating larger size particles produces fewer particles. The following sentence is added.

400 Section 2.3: *The choice of this size allowed us to generate the maximum number concentration of monodisperse particles.*

_ (6,177) space betwen RHw and conditions
Reply: Corrected.

405 _ (6,180s) **See my comment** above with regard to the **OPC spectra and interpretation** based on water droplet size predictions. Also, as a reader it became confusing that the authors switched from discussing droplet radius to droplet diameter when they begin discussing OPC data. **I suggest** that one dimension is chosen and all discussions and figures converted to this for consistency.
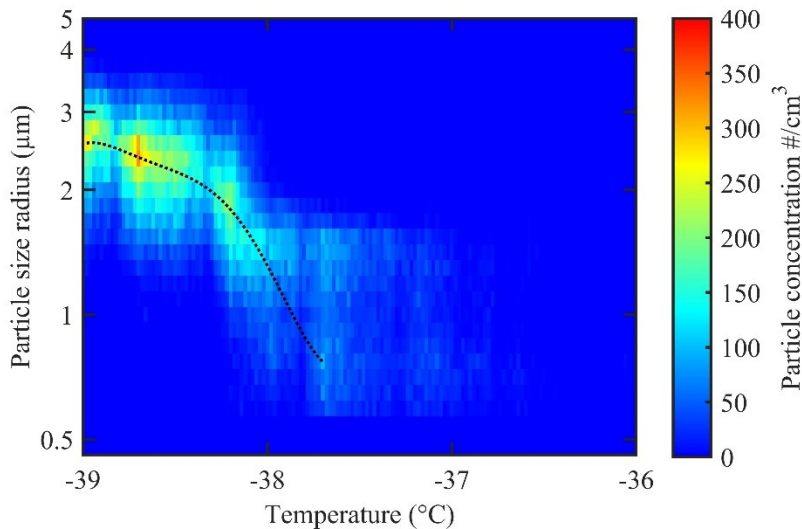**Reply**: The comments regarding ice crystal size and the relationship between droplet and ice crystal size related
410 to the nucleation section temperature are addressed above.
We revised Figure 5a such that Yaxis shows the particle units in radius, and it is now consistent with the other figures.

The following figure is added.
415

Figure 5: Homogenous freezing of water droplets containing one wt. % ammonium sulfate solution. (a) OPC classified ice particle concentrations as a function of ice crystal diameter at different temperatures. Warm and cold walls of the conditioning section are maintained at -9 and -27°C, respectively.

420
_ (6, 183) How are ice particles of 2.0 _m observed, when previously it was stated a cutoff of 3 _m is used to select ice? Is this a result of my radius versus diameter confusion?
Reply: The cutoff of 3 µm is defined in diameter. The new sentence in section 2.1 reads as

12

425   Section 2.1: … *certain size-threshold (≈3 µm **in diameter**).*

We also revised the cut size definition in section 2.3. The new sentence in section 2.3 reads as

Section 2.3: … *we observe ice particles of size ≈ 2.0 µm **in diameter**.*
430

_ (7, 200) "It can be seen that RHw values close to 113% are required before all the AS particles
are activated to droplets." I believe the observation is of ice, not of droplet activation. The DRH of
ammonium sulfate is _ 82% and weakly dependent on temperature. Thus all ammonium sulfate
particles should activate at much lower RH. The value of RH here is what is needed for them to grow
435   to a size, subsequently freeze, and remain big enough to be measured as ice.
       Reply: Agree. The sentence is revised as follows. The original sentences that follow this sentence discuss the
       importance of high RHw conditions.

Section 2.3: *It can be seen that RHw values close to 113% are required before all the AS particles are activated to*
440   *droplets **and measured as ice crystals** (Figure 5b).*

_ (7, 207) Here again another size 400 nm mobility diameter particle is used, perhaps a word as to
why this choice was made, relative to the 200nm or 300 nm used in other contexts in the text?
Reply: Following words to the existing sentence are added.
445

Section 2.4: Laboratory measurements showed that the contribution of double and triple charged particles was
less than 7 and 3%, respectively, **which also justified the choice of 400 nm size particles.**

_ (7, 211) 7% and 3%
450   **Reply**: Corrected.

_ (7, 222) was once .....is now
Reply: Corrected.

455   _ (7, 225) I suggest the authors stick with SI units – mph to m/s.
Reply: Corrected.

_ (8, 232) particles were also collected.... Were the same particles collected on the SEM films after
the CFDC or was this sampling run in parallel?
460   **Reply**: It was run in parallel. Highlighted words are added, and the existing sentence is revised as follows.

Section 2.4: **In parallel to INP measurements,** the particles were collected on a carbon type-B film (Ted Pella Inc.;
01814-F) for scanning electron microscopy-energy dispersive x-ray spectroscopy (SEM-EDS) analysis to better
understand the size distribution and composition of these airborne dust particles.
465

_ (8, 252) froze at the highest
Reply: Corrected.

470   _ (9, 263) See previous comment related to temperature ramping.
Reply: This comment is addressed above. See new figure Figures S8 caption.

Figure S8: *The F_{ice} of airborne arable dust species as a function of temperature and nucleation section cooling rates. The cooling rate of 0.5 Kmin^{-1} was used in this study.*

475   _ (9, 265) allows a comparison with other....
Reply: Corrected.

_ (9, 271) But citations in order from earliest to latest.
Reply: Corrected.

480

_ (9, 278) Here error in n_s is mentioned but does not lead to any uncertainty plotted in Figure 7. In addition to the error bars plotted from other studies it would be nice to have error bars plotted for this study.
Reply: The errors are plotted but they are invisible in the figure. For example, for K-Feldspar species, the n_s value
485   at -22°C is 0.1083x10^{12} (m^{-2}) and the error is 1.613x10^7 (m^{-2}).

_ (11, 339) Perhaps the authors could spend some more time attempting to explain why their results seem to be systematically high relative to the other studies (Figure 7). Are there good physical explanations for this?
490   **Reply**: In addition to the different measurement methods that might have led to this discrepancy (already discussed in the main paper); it is also possible the experimental uncertainties from different ns parameters (e.g. ice crystal detection limit, RH, and temperature error limits) could also influence the ns calculations. The following sentence is added.

495   Section 3: *The experimental uncertainties (e.g. ice crystal detection limit, RH, and temperature error limits) from these methods could also influence the n_s results.*

_ (conclusion) From the conclusions I am missing a discussion of whether other existing CFDCs could employ this technique. What for example are the physical constraints in terms of evaporation
500   section length? Given the published geometries of instruments like ZINC2, SPIN3 etc. could these instruments hope to run using the operational mode introduced here? Alternatively, if new chambers were being designed what features should be introduced or geometry utilized to enable operation in both traditional and this new mode? Recommendations to the community would strengthen the paper.
505   **Reply**: Yes, other CFDC's could employ this new method. Based on CFD results (Fig.S3-5), the minimum evaporation/nucleation length required is 0.2 m. Implementing a separate refrigeration system to independently cool the nucleation section, the new operation mode can be adapted. For a new chamber geometry, the length of the conditioning section can be increased such that droplet size can be increased. This feature is useful such that the lifetime of the ice layer can be increased because higher RHw = 113% is not needed.

510   The following sentences are added to section 3.

Section 3: *Our results can guide design considerations for future CFDC-style ice chambers. The length of the conditioning section can be increased so that higher RHw would not be necessary to activate all the particles to sufficiently large droplet sizes (≈ 2 μm in diameter). This design feature could help to increase the lifetime of the ice layer. Based on CFD results (Fig.S3-5), the minimum evaporation/nucleation length required is 0.2 m. Also,*
515   *implementing a separate refrigeration system to independently cool the nucleation section, the presented new operation mode can be adapted.*

_ (Figure 1) Can basic chamber dimensions be included, space appears plentiful.
Reply: We added the following sentence to the figure caption of Figure 1.

520   Figure 1: *The length of both the conditioning and nucleation section is 0.45 m. The width of the chamber is 0.15 m. The gap between warm and cold walls is 0.01 m.*

_ (Figure 2) Why include temperature from when initial cooling began? Why not just the shaded region, or shaded plus rewarming?
525   **Reply**: This is shown to give an idea of temperature time-series from the beginning of the experiment.

_ (Figure 5a) See previous comment with regard to radius versus diameter. Also, why the arbitrary scale? Is this a result of OPC binning? Can scale be changed to be linear? This plot is very hard to interpret in its current form.
530   **Reply**: Figure 5a is revised, please see above. A new figure is added that shows the Y-axis in particle size in radius units.
The scale is fixed. It was plotting typo. Adopting a linear scale makes the figure difficult to analyze. The new figure is clearer.

535   _ (Figure 6 caption) Suggest a change in text: Other solid square markers represent data collected when the chamber was operated in a steady-state temperature mode (instead of steady cooling).
Reply: Thanks for the suggestion. The sentence is revised.

Summary:
540   I have enjoyed reading the submitted manuscript and find that this is an intriguing new idea. In order to recommend the manuscript for publication I think the authors **need to state more convincingly** that they constrain the conditions for the observed nucleation. Furthermore, I think the conclusion would be significantly enhanced by describing **whether or not other existing CFDC systems** could run or test run such a mode of operation. I also encourage the authors **to conduct a round of editing** to ferret out
545   small mistakes that I found numerous enough that not all could be included here.
Reply: Thanks for these comments. The ice fraction is defined, see Text S1. The design recommendations for future CFDC chamber development are described in section 3. English editing was performed.

_

550   [1] Castar`ede, D. and Thomson, E. S. (2018). A thermodynamic description for the hygroscopic

15

growth of atmospheric aerosol particles. Atmospheric Chemistry and Physics, 18(20):14939–14948.

[2] Stetzer, O., Baschek, B., Lueoeond, F., and Lohmann, U. (2008). The zurich ice nucleation chamber (zinc) - a new instrument to investigate atmospheric ice formation. Aerosol Science and Technology, 42(1):64–74.

[3] Garimella, S., Kristensen, T. B., Ignatius, K., Welti, A., Voigtländer, J., Kulkarni, G. R., Sagan, F., Kok, G. L., Dorsey, J., Nichman, L., Rothenberg, D. A., Rösch, M., Kirchgäßner, A. C. R., Ladkin, R., Wex, H., Wilson, T. W., Ladino, L. A., Abbatt, J. P. D., Stetzer, O., Lohmann, U., Stratmann, F., and Cziczo, D. J. (2016). The spectrometer for ice nuclei (SPIN): an instrument to investigate ice nucleation. Atmospheric Measurement Techniques, 9(7):2781–2795.

555

560

565

570

575

580

16

Dear Reviewer,

Thanks for providing these comments to further improve the manuscript. Apologies for the delayed response, the last few months have been challenging during this pandemic. Please find below the reply to your comments. These comments are also used to revise the manuscript.

Thanks,

Gourihar Kulkarni

Anonymous Referee #RC3

Received and published: 16 March 2020

The Kulkarni et al, study describes a newly developed operating procedure for investigating the immersion freezing mechanism using continuous flow diffusion chambers. The new method converts the typical nucleation section of such chambers into a "conditioning" section where the aerosol particles are activated into cloud droplets at a fixed temperature where no freezing is expected. Then the particles transition into the newly dubbed "nucleation section" (formerly known as the evaporation section), which is cooled continuously while maintaining ice saturation. The newly developed technique compares well with previously published immersion freezing methods, although it appears to produce higher frozen fractions (within an order of magnitude) than previously observed for several dust species. I find the new method to be well implemented and a nice addition to the ice nucleation measurement community. I support this manuscript for publication and have the following comments:

General comments:

The residence time of the instrument is described as _10 seconds, yet the actual nucleation section is only half of that. This is not that different from traditional CFDCs, however, when the lifetime of the evaporating droplet in the nucleation section is considered, the nucleation time seems closer to _2 seconds (according to the numerical simulations). This should be noted in the text.

Reply: Following sentence is added. The word 'particle' is added to say that total particle residence within the chamber is ~ 10 s.

Section 2.1: …which limits the total **particle** residence time to ≈10 s. The droplet residence and nucleation time within the chamber are a maximum of 6.5 s and 2 s, respectively.

Furthermore, when considering that the droplets evaporate so quickly, is it possible to retrieve some information about nucleation rates based on the observed ice crystal sizes as a function of temperature, as was alluded to for the homogeneous freezing experiments?

Reply: This is another way of expressing INP measurements (Herbert et al. 2014). We know the ice fraction and particle surface area; however, nucleation time is uncertain. These inputs can be used to calculate the nucleation rate (J_{het}). Alternatively, a normalized freezing rate (R/A) can be calculated. We hope to provide the raw data upon request, and this data information would allow readers to calculate these rates.

Herbert, R. J., Murray, B. J., Whale, T. F., Dobbie, S. J., and Atkinson, J. D.: Representing time-dependent freezing behaviour in immersion mode ice nucleation, Atmos Chem Phys, 14, 8501-8520, 10.5194/acp-14-8501-2014, 2014.

Throughout the text, the new method was described as "the new method". I think it would be nice if the new technique had a name for easier future reference.

Reply: We call this new technique as 'Modified Compact Ice Chamber' or 'MCIC.' The manuscript is revised, and sentences are revised to incorporate MCIC.

Section 2.1: *Figure 1 shows a vertical cross-sectional geometry of the modified mode PNNL ice chamber,* **which is now referred to as a Modified Compact Ice Chamber (MCIC).**

Section 2.4: *The immersion freezing efficiency of K-feldspar, illite-NX, Argentinian soil dust, and airborne arable dust particles was measured to test the performance of the* **MCIC**.
Section 3: *A good agreement with the results obtained from* **MCIC** *was observed, …*

Section 3: *….4 up to 5 is needed to apply to the CIC-PNNL data to match with the data from the* **MCIC**.

Section 4: *An alternative method of operating a CFDC-style ice chamber* **referred as MCIC** *was explored to …*

I appreciate that the authors did a thorough evaluation of the instrumental design using CFD and pulse experiments. However, I found the description and justification of the settings used missing, see my comment below.

Although the authors go in depth in their comparison with the dusts tested with previous results, I found the justification for the observed differences to be rather vague. This is especially true when comparing with the observations from the FIN workshop where to my understanding, the same aerosols were being tested at the same time. Therefore it would be nice if the authors expanded on some of the reasoning as to why the results in ns can differ by up to an order of magnitude. For example, is it due to not all particles being activated in other techniques due to lamina issues or perhaps it is due to the
conditions that the droplets are evaporating at (warm wall temperature or cold wall temperature) etc.?

Reply: In addition to the different measurement methods that might have led to this discrepancy (already discussed in the main paper); it is also possible the experimental uncertainties from different n_s parameters (e.g. ice crystal detection limit, RH and temperature error limits) could also influence the n_s calculations. Following sentence is added.

Section 3: *The experimental uncertainties (e.g. ice crystal detection limit, RH, and temperature error limits) from these methods could also influence the ns results.*

Technical and minor comments:

Line 38-39: There is mounting evidence that the traditional view of deposition nucleation,
may not be occurring. As referenced in the cited Vali et al., (2015) deposition

nucleation has also been referred to as immersion freezing in pores or pored condensation and freezing (Marcolli, 2014). Consider adding pore condensation and freezing as a heterogeneous nucleation mechanism.

670 **Reply**: Following sentence is added.

Section 1: *Deposition nucleation has also been referred to as pore condensation and freezing mechanism because it is similar to as immersion freezing but in pores (Marcolli 2014).*

675 Line 53-54: Consider adding Garimella et al., (2017) as a reference as well.
Reply: Added.

Line 57 and 60-61: Did you test to see if all particles did indeed activate as droplets?
Reply: This was tested by freezing the droplets at and below homogeneous freezing temperatures. See Figure 5b.

680

Line 77: Are there two sheath flows of 5 lpm of was the total sheath flow 5 lpm? Please clarify.
Reply: There is one sheath flow. The existing sentence is revised.

Section 2.1: The **single** sheath and sample flow rates were 5 and 1 liters per minute (LPM), respectively, …

685

Line 78: With such a high supersaturation and the required temperature gradient to achieve this supersaturation, how can you ensure that all particles activated as droplets?
Reply: This was tested by freezing the droplets at and below homogeneous freezing temperatures. See Figure 5b.

690 Line 91-93: Here the temperature gradient between the walls is mentioned and the achieved temperature of -20 C is described in the following sentence. However, it may be worthwhile to specify the supersaturation of the conditioning section here as well (113 % RHw?).
Reply: Following sentence is added.

695 Section 2.1: *The resulting water and ice saturation conditions are shown in Figure 3.*

Line 99-102: This should be reworded, consider something like: "The isothermal conditions of the nucleation section is maintained at ice saturation and cooled at a steady rate (0.5_C min-1 100) by a separate cooling bath in order to determine the immersion freezing efficiency of INPs as a function of supercooled temperature"

700 **Reply**: Thanks for the suggestion. The sentence is revised as follows.

Section 2.1: *The isothermal conditions of the nucleation section is maintained at ice saturation and cooled at a steady rate (0.5°C min^{-1}) by a separate cooling bath to determine the immersion freezing efficiency of INPs as a function of supercooled temperature.*

705

Line 102-103: Why does the experiment proceed so far below the homogeneous freezing temperature?
Reply: The experiment could have terminated at the onset of homogeneous freezing temperature (-38 to -39 °C). Cooling below this temperature allowed us to obtain measurements at homogeneous freezing temperature for

19

~10 minutes. This additional data helped towards quality control and to account for the uncertainty within the temperature. The following sentence is added.

Section 2.1: *This additional supercooling below the onset of homogeneous freezing temperature allowed to obtain freezing data that was used towards data quality control and to account for the uncertainty within the temperature.*

Lines 110-112: Was there any gradient applied to the conditioning experiment during the pulse experiments? I find this unclear in the text. Furthermore, if a temperature gradient was applied in the conditioning section, are there any effects from the ice coating/ moisture from the walls on the buoyancy profile of the air in the chamber that are missed by doing the test without an ice coating? Also, are there any impacts on the lamina of the chamber when going from the conditioning section to the nucleation section when there is a temperature gradient of 22 C (-20 to -44 C)?

Reply: There was no gradient applied to the conditioning section of the chamber.
Flow conditions across the chamber are laminar (see Fig. 4a). The INP trajectory determined by the various forces (flow conditions and gravity) acting on the particle follows the fluid flow streamlines. Figure 3 shows the steady-state airflow velocity within the conditioning section of the chamber. These results indicate that the chamber conditions do not affect the buoyancy profile of the air. Therefore, particle pulse experiments are also valid after ice coating.

Figures S2-5 show no effect of the temperature gradient between the conditioning and nucleation section temperature on the aerosol lamina within the conditioning section and transitioning zone.

Line 183: remove "either" before "do"
Reply: Corrected.

Line 184-186: Please clarify these sentences. Are the smaller droplets at higher temperatures due to the lower nucleation rate and therefore the droplets evaporate more than at colder temperatures where nucleation is faster?

Reply: The droplet evaporation is observed from -20 till -37.5°C, see Figures S2 – 4. These figures show that droplets evaporate at the entrance of the conditioning section. E.g. Fig S3 c show that water droplet of size greater than 2 µm in radius will mostly contribute towards nucleation of ice. Droplets smaller than this size are exposed to subsaturation conditions, and they evaporate quickly (< 1 sec; see Fig S3 b). It should be noted that as nucleation occurs in the order of a few ms (Holden et al. 2019), the droplets smaller than 2 µm might also contribute towards nucleation of ice. However, the contribution of these smaller droplets of less than 2 µm is very small (see Fig. 5a).

Line 183: Remove "the" between "of" and "supercooled"
Reply: Corrected.

Lines 191-195: seem to be contradicting each other, consider rewording.
Reply: The sentences are revised as follows.

Section 2.3: *We find good agreement between the experimental and predicted freezing temperatures. These results also show the complete evaporation of supercooled droplets within the nucleation section, because no ice particles are observed above ~≈ 37.5°C, and therefore the freezing results (see section 3) at warmer temperatures (> -37°C) can be ascribed as the heterogeneous freezing of the droplets or immersion freezing.*

Line 200-224: Consider breaking this sentence in two for easier readability.
Reply: The sentence is divided into two sentences for clarity.

Section 2.3: *Higher RHw values enable the encapsulation of all particles that are within and may spread outside (Garimella et al. 2017) the width of aerosol lamina into droplets. **In addition,** high saturation conditions also help to grow the droplets to the larger size; so, they survive long enough to induce the freezing of droplets within the nucleation section.*

Line 206: Rather than stating "a new mode" perhaps consider stating that it is operated in this specific mode (name the mode).
Reply: We call this new technique as 'Modified Compact Ice Chamber' or 'MCIC.' The manuscript is revised, and sentences are revised to incorporate MCIC.

Line 223-224: Consider rewording.
Reply: The sentence is revised as follows.

Section 2.4: The region was once covered with basalt lava, but is now built up with loose topsoil – loess.

Line 245-246: Earlier, it is stated that an experiment ends at -44 C yet now the experiment ends at -38, which makes more sense, be sure to be consistent.
Reply: Sorry for the confusion. Although the experiment ends at -44°C, the INP data from -20 to -38°C is only investigated and presented in this study.

References
Garimella, S., Rothenberg, D. A., Wolf, M. J., David, R. O., Kanji, Z. A., Wang, C., Rösch, M. and Cziczo, D. J.: Uncertainty in counting ice nucleating particles with continuous flow diffusion chambers, Atmos Chem Phys, 17(17), 10855–10864, doi:10.5194/acp-17-10855-2017, 2017.

Marcolli, C.: Deposition nucleation viewed as homogeneous or immersion freezing in pores and cavities, Atmos Chem Phys, 14(4),2071–2104, doi:10.5194/acp-14-2071-2014, 2014.

Vali, G., DeMott, P. J., Möhler, O. and Whale, T. F.: Technical Note: A proposal for ice nucleation terminology, Atmospheric Chem. Phys., 15(18), 10263–10270, doi:10.5194/acp-15-10263-2015, 2015.

A new method for operating a continuous flow diffusion chamber to investigate immersion freezing: assessment and performance study

Gourihar Kulkarni[1], Naruki Hiranuma[2], Ottmar Möhler[3], Kristina Höhler[3], Swarup China[1], Daniel J. Cziczo[4], Paul J. DeMott[5]

[1]Atmospheric Sciences and Global Change Division, Pacific Northwest National Laboratory, Richland, WA, USA
[2]Department of Life, Earth and Environmental Sciences, West Texas A&M University, Canyon, TX, USA
[3]Karlsruhe Institute of Technology (KIT), Institute of Meteorology and Climate Research (IMK-AAF), Eggenstein-Leopoldshafen, Germany
[4]Earth, Atmospheric and Planetary Sciences, Purdue University, IN, USA
[5]Department of Atmospheric Science, Colorado State University, Fort Collins, CO, USA

Correspondence to: Gourihar Kulkarni (Gourihar.Kulkarni@pnnl.gov)

Abstract. Glaciation in mixed-phase clouds predominately occurs through the immersion freezing mode where ice nucleating particles (INPs) immersed within supercooled droplets induce nucleation of ice. Currently, Mmodel representations of this process currently are a large source of uncertainty in simulating cloud radiative properties, and to constrain these estimates, continuous flow diffusion chamber (CFDC)-style INP devices are commonly used to assess the immersion freezing efficiencies of INPs. In this study, a new approach was explored to operating such an ice chamber that provides maximum activation of particles without droplet breakthrough and correction factor ambiguity to obtain high-quality INP measurements in a manner that has not been demonstrated as possible previously. The conditioning section of the chamber was maintained at ≈~≈-20°C and water relative humidity (RH_w) ~≈113% conditions to maximize the droplet activation, and the droplets were supercooled with an independently temperature-controlled nucleation section at a steady cooling rate (0.5°C min^{-1}) to induce the freezing of droplets and evaporation of unfrozen droplets. The performance of the modified ice chamberModified Compact Ice Chamber (MCIC) was evaluated using four INP species: K-feldspar, illite-NX, Argentinian soil dust, and airborne arable dustsoil dusts from an arable region that had shown ice nucleation over a wide span of supercooled temperatures. Dry dispersed and size-selected K-feldspar particles were generated in the laboratory. Illite-NX and soil dust particles were sampled during the second phase of the Fifth International Ice Nucleation Workshop (FIN-02) campaign, and airborne arable soil dust particles were sampled from the aerosol inlet located on the rooftop of the laboratoryan ambient aerosol inlet. The measured ice nucleation efficiencies of model aerosols with a surface active site density (n_s) metric were higher, but mostly agreed within one order of magnitude compared to results reported in the literatureliterature results.

1   Introduction

Atmospheric ice nucleation plays an important role in initiating precipitation in clouds that consist of a mixture of supercooled liquid water droplets and ice crystals and in catalyzing the formation of ice particles within high-altitude cirrus clouds (Lohmann and Feichter, 2006; Boucher et al., 2013). This important step toward ice formation also affects the lifetime and

22

radiative properties of these clouds; however, ice nucleation mechanisms are poorly understood and parameterized in cloud models (e.g., Hoose and Möhler, 2012; Murray et al., 2012; Kulkarni et al., 2012; Kanji et al. 2017; Knopf et al., 2018). Homogeneous ice nucleation is responsible for the formation of ice particles in dilute water and supercooled solution droplets at temperatures lower than ~≈-38°C (Pruppacher and Klett, 1997). Ice nucleation can also proceed through heterogeneous ice nucleation triggered by INPs (Vali et al., 2015). Multiple heterogeneous ice nucleation mechanisms have been proposed, such as deposition nucleation (ice formation on ice nucleating particles (INPs) directly from the vapor phase), contact freezing (freezing initiated by INPs the moment they come into contact with a supercooled droplet), and condensation and immersion freezing (freezing initiated by immersed INPs within the supercooled water or solution droplets). Deposition nucleation has also been referred to as pore condensation and freezing mechanism because it is similar to as immersion freezing but occurs in pores (Marcolli 2014). Nevertheless, the immersion freezing mode is thought to be the most important process toward for the formation of ice particles within mixed-phase clouds (e.g., Ansmann et al., 2009; Westbrook and Illingworth, 2013).

Immersion freezing measurements are commonly made using continuous flow diffusion chamber (CFDC) devices (e.g., Rogers, 1988; Chen et al., 1998; Stetzer et al., 2008; Kanji and Abbatt, 2009; DeMott et al., 2010; Friedman et al., 2011; Chou et al., 2011; Jones et al., 2011; Kanji et al., 2013; Boose et al., 2016; Garimella et al., 2016, Schiebel, 2017; Zenker et al., 2017). These chambers consist of two ice-coated "parallel" walls held at different temperatures, and different ice supersaturations are achieved by regulating the temperature gradient. Aerosols sampled into CFDCs are subjected to known discrete temperature and relative humidity conditions, and when the water relative humidity (RH_w) is more than a few percents above 100 percent%, droplets will activate on the majority of particles within the growth section of the chambers. CFDCs also then typically have an evaporation section located at the bottom of the chamber where the wall temperatures are controlled in order to evaporate the droplets that did not freeze. Frozen droplets are counted using an optical particle counter (OPC) to determine the atmospheric INP concentrations (Garimella et al., 2017). However, the maximum RH_w values achievable in this manner can limit the ability to determine the maximum immersion freezing fraction (DeMott et al., 2015).

Here, we have expanded the capabilities of the CFDC-style device in order to achieve the maximum activation of particles to detect the immersion freezing number concentrations of INPs at various supercooled temperatures. We present data to assess the performance from a newly developed CFDC in which all individual aerosol particles are activated to droplets, and these droplets are exposed to a spectrum sequence of supercooled temperatures. This is accomplished by modifying the existing design of the Pacific Northwest National Laboratory (PNNL) ice chamber (e.g., Friedman et al., 2011; Kulkarni at al., 2012). In the modified version, the growth section of the chamber was maintained at higher RH_w conditions at moderate supercooling to activate all aerosol particles to supercooled droplets, whereas the evaporation section was always held at ice-saturated conditions and cooled over a range of temperatures at a known constant rate. The evaporation section serves two purposes in this case: it induces freezing of droplets and evaporates the unfrozen droplets. Validation experiments using standard salt solutions are presented. Various INP proxies of mineral dust types that have previously shown ice nucleation ability over a wide span of supercooled temperatures were used to test the performance of the modified chamber.

2   Experimental Design and Performance Validation

2.1   Description of the existing and modified chamber

The PNNL CFDC-style ice chamber operated in the traditional mode, referred to as the Compact Ice Chamber (CIC)-PNNL, has been described ~~in the literature~~previously (e.g., Friedman et al., 2011; Kulkarni at al., 2012). The chamber consists of two sections: a growth section and an evaporation section joined together but thermally ~~insulated~~ isolated from each other. Each section consists of two parallel vertical surfaces that are both coated with a thin layer of ice, and these plates are independently temperature-controlled using external cooling baths (Lauda Brinkmann Inc.). Application of an ice layer ($\approx$0.5 mm thick) on these surfaces involved three consecutive steps: cooling the plates of the chamber to -25°C, filling the gap between the two parallel surfaces with deionized water ($\approx$18 MΩ cm), and expelling the water after 20 s. To produce the desired water- or ice-supersaturation conditions, a horizontal linear temperature gradient between the plates was applied, and the corresponding temperature and RH_w or relative humidity with respect to ice (RH_{ice}) were calculated using the Murphy and Koop (2005) vapor pressure formulations. The single sheath and sample flow rates were 5 and 1 liters per minute (LPM), respectively, resulting in a total particle residence of $\approx$10 s in the chamber. The temperature gradient was applied such that supersaturation conditions RH_w = $\approx$106% were achieved in order to investigate the immersion freezing efficiencies of both atmospheric and laboratory-generated INPs. An~~The~~ OPC (CLiMET, model CI-3100) was used to classify the particles as ice crystals if they were greater than a certain size-threshold ($\approx$3 µm in diameter). The ice fraction (F_{ice}) was calculated by taking the ratio of the ice crystal concentration classified by the OPC to the total condensation nuclei (CN) concentration that entered the chamber. The CN concentration was provided by a condensation particle counter (CPC; TSI 3775). Blank experiments using dry and filtered sample air were also performed at the beginning and end of each experiment for $\approx$10 minutes to calculate the background number of ice particles. Further, these ice particles were subtracted from the ice crystal concentration measured by the OPC, and the F_{ice} was corrected.

Figure 1 shows ~~a~~ the vertical cross-sectional geometry of the modified mode PNNL ice chamber, which is now referred to as a Modified Compact Ice Chamber (MCIC). This chamber design has a parallel plate CFDC-style geometry, whose principle of generating a supersaturation between the two "parallel" surfaces and determining the F_{ice} is similar to that of the existing CIC chamber, but with modifications as described here. The growth and evaporation sections of the CIC chamber are now referred to as conditioning and nucleation sections, respectively. The length of these two sections is identical (0.45 m), which limits the total particle residence time to $\approx$10 s. The droplet residence and nucleation time within the chamber is maximum 6.5 s and 2 s, respectively. –The chamber wall temperature values as a function of time during one typical ice nucleation experiment are shown in Figure 2. During our study, the temperature controller of the cooling thermostat was programmed such that the warm and cold wall temperatures of the conditioning section were set to -9 and -27°C, respectively. The resulting water and ice saturation conditions are shown in Figure 3. Here, the choice of conditioning section temperature was based on previous knowledge that the onset temperature of the INP test species being needed to induce nucleation of ice was at colder

24

temperatures (< -20°C) and the lower detection limit being needed to measure ice concentrations for temperatures warmer than -20°C. The shaded region shows the period (≈30 minutes) of one ice nucleation measurement, i.e., the OPC data from this period only are analyzed. The ice fraction (F_{ice}) now indicates the cumulative fraction of droplets frozen as a function of decreasing temperature of the nucleation section (see Text S12). This metric of reporting ice nucleation results is commonly used to report frozen fraction vs. temperature (F_{ice} vs. T) results (see e.g., DeMott et al., 2018; Kanji et al. 2017; Kohn et al. 2016). The isothermal conditions of the nucleation section is maintained at ice saturation and cooled at a steady rate (0.5°C min^{-1}) by a separate cooling bath in order to determine the immersion freezing efficiency of INPs as a function of supercooled temperatureThe isothermal conditions of the nucleation section always help to maintain the ice saturation conditions and the complete section is cooled at a steady rate (0.5°C min^{-1}) by another separate cooling bath in order to determine the immersion freezing efficiency of INPs as a function supercooled temperature. The choice of steady-state cooling rate is empirical at this moment, and the experiment is terminated when the nucleation section reaches ≈-44°C. This additional supercooling below the onset of homogeneous freezing temperature allowed to obtain freezing data that was used towards measurement quality control and to account for the uncertainty within the temperature. The implications of higher cooling rates towards INP measurements were also explored. The particle residence time (≈5 s) and ice-saturated conditions of the nucleation section allow a sufficient size differential between supercooled droplets and ice crystals, and in fact, prevent "droplet breakthrough" (Stetzer et al. 2008). While keeping the conditioning section conditions constant, the temperature of the nucleation section is raised to ≈-20°C to prepare for the next ice nucleation measurement. This operation allows us to probe the immersion freezing efficiency of INPs at various temperatures (-20 to -44°C) multiple times (≈ 5) before another layer of ice coating is applied. After more than five ice nucleation measurements or after approximately 3 hours, we see the reduced F_{ice} of standard solution droplets (discussed below). The particle pulse experiments (Garimella et al. 2017) using size-selected 300 nm mobility diameter ammonium sulfate particles and ≈10.5 s pulse were performed. The temperature of the conditioning and nucleation sections were held constant at 20 °C, and the particle concentration at the chamber outlet using the CPC was measured. These measurements show that ≈16% of total particles that enter the chamber have moved outside of the lamina (Figure S1). Therefore, higher RH_w values are utilized in the chamber to activate these particles to droplets (see below). Simulations (see below) are performed to investigate the sensitivity of polydisperse particles. The particle residence time of three different monodisperse particles (0.3 μm, 1.0 μm, and 2.0 μm) traversing the chamber were calculated (Figure S1). Results show that the residence time of these particles are similar indicating monodisperse size pulse experiments are also applicable to other size particles. At the entrance of the nucleation section, the temperature and RH_w profiles can be unsteady, and to better understand the flow patterns of these profiles within the transitioning zone, and its impact on droplet behavior, numerical simulations using computational fluid dynamics (CFD) are performed (as discussed below).

2.2   Numerical modeling

At the entrance of the nucleation section, the temperature and RH_w profiles can be unsteady, and to better understand the flow patterns of these profiles within the transitioning zone, and its impact on droplet behavior, numerical simulations using

computational fluid dynamics (CFD) were performed. In this study, the warm and cold walls of the conditioning section were maintained at -9 and -27°C, respectively, and the nucleation section was maintained at -20°C. Analytical steady-state calculations based on Rogers (1988) were also used to understand the nature of the flow velocity profile and the position of the aerosol lamina occupied between the warm and colder walls (Figure 3). The results show that the operating conditions of the chamber produce a skewed velocity profile and that the aerosol lamina is displaced toward the colder wall. The aerosol lamina is surrounded by filtered sheath flow, and its width is determined by the ratio of sample to sheath airflow. Because sample flow ideally occupies this fraction of the total flow, the aerosol lamina experiences a range of temperature and saturation conditions. The center temperature and RH_w conditions, including uncertainty across the aerosol lamina (assuming ideal confinement in the lamina), are $\approx$-19.7 ± 0.7°C and $\approx$113 ± 0.5%, respectively. Additional simulations are performed to understand the center temperature and RH_w conditions required to confine the particles that are moved out of the aerosol lamina. We find that the revised uncertainties for center temperature and RH_w conditions are ± 0.9°C and ± 0.7%, respectively.

CFD simulations are were performed to achieve a complete description of the velocity, ice saturation, and temperature conditions within the chamber (Figure 4a). A three-dimensional mesh of the chamber geometry was generated and exported to the commercially available CFD software ANSYS FLUENT 14.0 (2016). The CFD software solver was the pressure-based steady-state Navier-Stokes equation, which has with implicit and absolute velocity formulations. We used the RNG κ – ε turbulence models, which treat velocity fluctuations better than other turbulence models for such geometry, and it was coupled with energy and viscous heating to enable the species transport model to better capture the effects of smaller eddies of fluid motion The viscous model – the standard RNG κ – ε turbulence model was used. This model treats velocity fluctuations better than other turbulence models for such a geometry. This turbulence model was used in conjunction with species transport modeling capability such that effects of smaller eddies of fluid motion are better captured. The pressure outlet boundary condition was used, as were the CFD solution method to couple the pressure-velocity, and the default SIMPLE scheme used. The Lagrangian discrete-phase model was used to simulate the potential INP trajectories released from the sample injection region to the outlet end of the chamber. The simulations were performed using an "uncoupled approach," which means the motion of INP particles does not influence the fluid flow pattern. The temperature and RH_w fields of the INP trajectories were used to calculate the droplet growth and evaporation trajectories using a water vapor diffusion growth theory (Rogers and Yau, 1988) that neglects temperature corrections and kinetic and ventilation effects and assumes perfect mass and thermal accommodation coefficients (Text S2+).

The CFD simulated airflow velocity and RH_{ice} profiles from the central region of the conditioning section are nearly similar to the analytical solution (Figure 4a2). Both calculations show the presence of maximum humidity values near the middle of the chamber but slightly displaced values toward the cold wall. The fluid flow temperature characteristics from the moment the aerosol lamina joins the sheath flow show that the aerosol sample quickly (<0.5 s) cools at the entrance of the conditioning section. To gain a better understanding of RH_w and temperature conditions within the conditioning and nucleation sections, the simulated data set of a potential INP trajectory transiting within the chamber is shown (Figure 4b). The potential INPs

experience nearly constant RH_w and temperature conditions within a short time, ≈1 s, after entering the conditioning section. The potential INPs are assumed (i.e., sub-saturated particle growth is ignored) to activate to droplets because they are greater than cloud ~~condensation nuclei~~CN sizes (Seinfeld and Pandis, 2016) and grow as long as RH_w is increasing or remains constant. As the INPs enter the nucleation section, their RH_w and temperature values equilibrate with the nucleation section conditions. These calculations show that the droplets grow to ≈4 μm in diameter, and they shrink as RH_w and temperature decrease (within the nucleation section). Note that droplet freezing within the nucleation section is not simulated in these simulations. Additional simulations with the nucleation section temperature set to -30°C and -37.5°C were also performed (Figure S2-5). These simulations show that the RH_w field of a potential INP slightly decreases ($\approx0.5\%$) and then increases within a very short period of time (<0.5 s) at the entrance region of the nucleation section. However, calculations show that such a perturbation does not affect the droplet evaporation behavior within the nucleation section as they all evaporate within ≈1s after they enter the nucleation section and within uncertainty limits of set temperature of the nucleation section, but not before they reach the set temperature (see Figures S2-4). The simulations are extended to understand the RH_w and temperature conditions of potential INPs released from different regions of the inlet section of the chamber. Simulations of five potential INPs are shown in S5. It is observed that INPs experience various temperature conditions (-17 to -19.5°C) within the conditioning section, however, after ≈0.5s they all enter the nucleation section the temperature of each trajectory is identical.

Additional evaporative cooling calculations ~~are~~ were performed to understand the suppression of droplet temperature while they are enter~~ing~~ the nucleation section. In the nucleation section the supercooled droplets experience sub-saturation ($RH_w >$ 0.8) and colder temperature conditions (> -37.5°C). The Kulmala evaporative model (Su et al. 2018) was used to determine the surface temperature of these droplets using steady-state aerosol lamina airflow velocity (Figure 3) and theoretical predicted RH_w fields (Figures S2-4). The calculations (Table S1) show the negligible effect of evaporative cooling on the droplet temperature such that additional supercooling is within the reported temperature uncertainty ($= \pm 0.7$°C) across the aerosol lamina, and therefore ~~droplet~~ evaporating droplet cooling effects within the nucleation section are ignored.

2.3   Homogeneous freezing of ammonium sulfate particles

The temperature conditions within the nucleation section were validated using size-selected ammonium sulfate (AS) particles. These particles were generated by atomization of an aqueous solution made by dissolving AS (1 g) and Milli-Q water (18.2 MΩ cm; 100 g) and resulting in a 1 wt% solution concentration using a constant output atomizer (TSI 3076). The atomized droplets were transported through a diffusion drier to obtain the dry particles, which were further transported to the differential mobility analyzer (DMA; TSI 3081) to obtain size-selected particles that had mobility diameters of 200 nm. The choice of this size allowed to generate maximum number concentration of monodisperse particles. The concentration of these size-selected particles was measured using a CPC, and the particles were further transported to the ice chamber. As stated previously, the temperature and RH_w conditions within the conditioning section were -20°C and $\approx113\%$, respectively, and these conditions were held constant, which led to droplet activation of size-selected AS particles. Next, the nucleation section was steadily

27

cooled from -20 to -40°C, and the ice particles exiting the chamber were classified as ice particles. The ice particle size distribution with supercooling is shown in Figure 5a. The results show that the droplets began to freeze via a homogeneous freezing mode at $\approx$-37.5°C. The maximum number of ice particle concentrations was observed at $\approx$-38.5°C when all the droplets froze. The nucleation section is always maintained at RH_{ice} = 100% (see Figure 4a), and such ice saturation conditions either do not grow or sublimate the ice crystals. Therefore, ice particle size measured by the OPC can be representative of the size of the droplet while freezing. At slightly warmer temperature (between -38.5 and -37.5 °C), we observe ice particles of size $\approx$ 2.0 µm in diameter. The appearance of these smaller ice crystals could be because of the freezing of these smaller droplets (a consequence of evaporation within the entrance zone of the nucleation section) compared to $\approx$ 5.0 µm droplets at $\approx$-38.5°C. These homogeneous freezing threshold temperature values are in agreement with previous studies (e.g., Ignatius et al., 2016; Kohn et al., 2016). For example, Kohn et al. (2016) found 100% freezing of the supercooled dilute aqueous solution droplets at $\approx$-38.2°C. Theoretical calculations using a homogeneous nucleation rate (e.g., Earle et al. 2010; Atkinson et al. 2016) were performed to predict the homogeneous freezing curves of the droplet of size 4 µm in diameter. Homogenous freezing curves for various probable droplet residence times within the nucleation section are shown in Figure S6. Note the good agreement between the experimental and predicted freezing temperatures. These results also show the complete evaporation of supercooled droplets within the nucleation section, because no ice particles are observed above $\approx$ 37.5°C, and therefore the freezing results (see section 3) at warmer temperatures (> -37°C) can be ascribed as the heterogeneous freezing of the droplets or immersion freezing. We find good agreement between the experimental and predicted freezing temperatures, and the freezing results (see section 3) at warmer temperatures (> -37°C) can be ascribed as the heterogeneous freezing of the droplets or immersion freezing. Our results also show the complete evaporation of supercooled droplets within the nucleation section, because no ice particles are observed above ~ 37.5°C.

This experimental setup was further applied to understand the relationship between the F_{ice} of AS particles relative to the RH_w conditions within the conditioning section. The aim was to investigate the RH_w value at which all the size-selected AS particles activate to droplets. Here, the nucleation section was held at -42°C to induce homogeneous freezing of solution droplets, while the RH_w within the conditioning section was steadily increased. It can be seen that RH_w values close to 113% are required before all the AS particles are activated to droplets and measured as ice crystals (Figure 5b). Higher RH_w values enable the encapsulation of all particles that are within, and may spread outside of (Garimella et al. 2017) the width of aerosol lamina into droplets (Garimella et al. 2017). In addition, but high saturation conditions also help to grow the droplets to the larger size; so, they survive long enough to induce the freezing of droplets within the nucleation section.

2.4   Sample preparation

The immersion freezing efficiency of K-feldspar, illite-NX, Argentinian soil dust, and airborne arable dustsoil dusts from arable region particles was measured to test the performance of the ice chamber operated in a new modeMCIC. K-feldspar (BCS376) was purchased from the Bureau of Analysed Sampled Ltd, UK. Dry dispersed (TSI 3433) K-feldspar particles that

28

had a mobility diameter of 400 nm were size-selected by a DMA, and these nearly monodisperse particles were transported to the CPC and ice nucleation chamber. Based on theoretical calculations (Baron and Willeke, 2001), the distribution of these classified particles may also contain sub-populations of double (~≈700 nm) and triple (~≈985 nm) charged particles. Laboratory measurements showed that the contribution of double and triple charged particles was less than 7% and 3%, respectively, which also justified the choice of 400 nm size particles. Therefore, the multiply charged particle contribution is neglectedignored, and the K-feldspar aerosol stream is assumed to consist only of particles whose mobility diameter equals 400 nm. However, the surface area of multiple charged particles could influence F_{ice}, because these large particles (>400 nm) provide larger surface areas (Lüönd et al., 2010). Illite-NX and Argentinian soil dust were sampled at the AIDA (Aerosol Interaction and Dynamics in the Atmosphere) chamber facility during the Fifth International Ice Nucleation Workshop (FIN-02) campaign (DeMott et al., 2018). During the campaign, the two aerosol types were dry dispersed in two different chambers: an 84 m^3 AIDA chamber and a 4 m^3 aerosol particle chamber (APC); but in this study, we sampled directly from the APC. The details of particle generation and aerosol properties are described by DeMott et al. (2018). The direct sampling of these two aerosol types corresponds to experiment numbers 8 and 10 on 3/16/2015 and 3/17/2015, respectively. Airborne soil dust from an arable region or shortly Aairborne arable dust particles were sampled at the PNNL sampling site during a regional windblown dust event. The PNNL sampling site is located within the Columbia Plateau, WA, the USA, which is confined by the Rocky Mountains to the east, the Blue Mountains to the south, and the Cascade Mountains to the west. The region was once was covered with basalt lava, but is now is built up with loose topsoil – loess. This fine soil, which is erodible, and the agricultural dryland farming practices make this dry soil susceptible to wind erosion. The sampling was performed during one dust event on 5/11/2017, and the average temperature, humidity, and wind speed during this day were 18°C, 60%, and 14 6.26 m/sph, respectively. The sampling port was ~≈9 m above the ground on the rooftop of the Atmospheric Measurements Laboratory located on the PNNL campus in Richland, WA. The airborne dust particles were drawn into the laboratory through a cyclone impactor (URG-200-30EH), which was operated at 30 LPM to obtain a cut point diameter equal to 1.5 μm. This size-selective sampling allowed for removal of the larger particles (>1.5 μm) and therefore helped to classify unambiguously the ice crystals larger than 3 μm using an OPC. The CN concentration of airborne arable dust particles (>0.1 μm) was measured using a laser aerosol spectrometer (LAS; TSI 3340). The F_{ice} was calculated by determining the ratio of ice crystals provided by the OPC to the CN counts measured by the LAS. In parallel to INP measurements, the particles were collected on a carbon type-B film (Ted Pella Inc.; 01814-F) for scanning electron microscopy-energy dispersive x-ray spectroscopy (SEM-EDS) analysis to better understand the size distribution and composition of these airborne dust particles. The films were mounted on the C-and D-stages of a SKC Sioutas impactor that had 50% cut-points of 0.5 and 1.0 μm, respectively. The impactor was operated at 9 LPM, and a total of 1183 particles were analyzed. Figure S7 shows the exemplary SEM images. The images reveal that the particles are mostly composed of minerals, and the size distribution shows the mean area equivalent diameter of ~≈0.53 μm. The input aerosol concentration of all four INP species varied from 100 to 800 # per cubic centimeters, and the sampling duration was ~30 minutes.

3   Results and Discussion

The ~~modified ice nucleation chamber~~MCIC was operated to measure the maximum immersion freezing fraction of INPs. The modified design allowed for the faster (~~~~≈ 30 minutes) accumulation of immersion freezing data points to develop a continuous representation of the immersion freezing behavior of INPs compared to the traditional CIC-PNNL design, ~~where~~ in which immersion freezing was investigated at discrete temperatures. These expanded capabilities were demonstrated by measuring the immersion freezing properties of four INP substances~~, including~~: K-feldspar, illite-NX, Argentinian soil dust, and airborne arable dust particles.

The measurements of immersion freezing properties of the four samples were investigated at temperatures between -20 and -38°C. The averaged F_{ice} data over $\Delta T = 0.25$°C temperature intervals were plotted against the midpoint temperature of each bin (Figure 6). The vertical and horizontal error bars are equal to the one standard deviation of the F_{ice} measurements (n = 3) and temperature uncertainty (± 0.4°C) across the nucleation section, respectively. Freezing experiments with AS solution droplets show the homogeneous freezing threshold temperature conditions below ~~~~≈-38°C, and therefore F_{ice} data points above this temperature can be attributed to the immersion freezing mode only. Figure 6 shows that four INP materials exhibit a distribution of immersion freezing temperatures. The F_{ice} of all INP species increased with decreasing temperature consistent with many past studies (e.g., Kanji et al., 2017). The droplets containing immersed K-feldspar particles froze at the higher temperatures. The median freezing temperatures (i.e., the temperature at which 50% of the droplets froze) of K-feldspar, illite-NX, Argentinian soil dust, and airborne arable dust particles was -25.4, -32.6, -31.4, and -31.8°C, respectively, and the difference between freezing temperatures corresponding to F_{ice} equal to 90% and 10% was approximately between ~~~~≈4.5 and 7.5°C for all four INP materials.

Additional experiments were performed to confirm that the dynamic temperature conditions (steady-state cooling) of the nucleation section does not affect the freezing behavior of particles. The measurements were conducted on K-feldspar and airborne arable dust particles that were prepared as described above in the sample preparation section. The temperatures of the warm and cold walls of the conditioning section were maintained at -9 and -27°C, respectively, and the nucleation section temperature was held constant (instead of steady-state cooling). The immersion freezing fraction data points of these two species are shown as solid symbols in Figure 6. ~~GA~~ good agreement with the results obtained ~~where the chamber was operated in a new mode~~from MCIC was observed, which suggests that the temperature ramping operation of the nucleation section (0.5°C min⁻¹) does not affect the performance of INP activation experiments. The experiments with higher cooling rates (2.5 and 7.0 °C min⁻¹) had negligible effects on F_{ice} of airborne arable dust species (Figure S8). Further, the time-dependent immersion freezing framework (e.g., Vali and Snider (2015), Herbert et al. (2014)) suggests that the rapid cooling of the droplets could shift the cumulative ice fraction towards the colder temperature based on the cooling rate and particular INP material constant. However, these input parameters for the time-dependent model are not available currently to quantify the

temperature shift for the present experimental conditions. Future studies that involves collocated direct and post-processing INP instruments would be needed.

These F_{ice} measurements were further analyzed using the ice nucleation active site density (n_s) approach that ~~allowed to compare against~~allows a comparison with other studies (see below). This approach also allowed us to compare results directly with literature data obtained using different experimental setups and various direct and post-processing INP instruments and particle generation methods. The n_s indicates the cumulative number of ice active sites that are present per unit area of particle surface, and that induce nucleation of ice upon cooling from 0°C to experimental temperature T. In this calculation, time-dependence is neglected, and it is assumed that the different active sites present within the droplets are responsible for the nucleation of ice. The n_s calculation follows ~~DeMott et al. (2018) and~~ Hiranuma et al. (2015) and DeMott et al. (2018):

$$n_s(T) = \frac{-\ln(1-F_{ice})}{A} \approx \frac{F_{ice}}{A} \tag{1}$$

where A is the surface area per particle, and the approximation is valid for $F_{ice} \ll 1.0$ in Eq. (1). For K-feldspar and airborne arable dust particles analysis, the surface area is calculated assuming the particles are spherical, and this assumption may overestimate the n_s; therefore, calculations should be viewed as the upper estimates of n_s. The size distribution and CPC concentrations were used to calculate the A of individual airborne arable dust particles, as described by Niemand et al. (2012). For illite-NX and Argentinian soil dust particles, the A was obtained from the FIN-02 data archive (DeMott et al., 2018). The error in n_s (Eq. 1) was calculated using the error propagation method based on the uncertainties of the F_{ice} and A.

Figure 7 shows n_s for the four INP materials tested in this work in comparison to parameterizations reported in previous studies. n_s for K-feldspar is compared to the fit published by Atkinson et al. (2013). There is a good agreement with our measurements for temperatures warmer than -26°C. Atkinson et al. (2013) used a droplet-freezing cold stage technique, ~~where~~in which a known amount of K-feldspar material was present in each droplet sized between 14 and 16 µm. These droplets were cooled at a rate of 1°C min^{-1}, and droplet-freezing temperature data were used to construct the n_s parameterization. Note that the n_s fit from Atkinson et al. (2013) is valid up to -25°C. In our work, we extrapolated the fit outside this limit to colder temperatures for comparison. However, such linear extrapolation to colder temperatures may not be correct, because, as both Niedermeier et al. (2015) and DeMott et al. (2018), the latter from the FIN-02 campaign, have shown, the n_s values level off at temperatures colder than -25°C. n_s for airborne arable dust was compared with the previous studies. Niemand et al. (2012) derived the n_s fit using combined immersion freezing data from various natural dusts (Asian soil dust, Canary island dust, Saharan dust, and Israel dust). Recently, Ullrich et al. (2017) developed n_s parameterization using immersion freezing n_s densities of various arable dusts (Saharan desert dust, Asian desert dust, Israel desert dust, Canary Island dust) for the temperature range from -14 to -30°C. Tobo et al. (2014) investigated the INP abilities of agriculture soils dusts collected from Wyoming, USA. Boose et al. (2016) investigated the INP efficiencies of airborne dust samples from four locations (Crete, Egypt, Peloponnese, and Tenerife) and generated the minimum to maximum bounds of n_s from -29 to -37°C. The comparison of our results with these previous results shows good agreement within one order of magnitude at colder temperatures, but the data diverge at warmer

31

temperatures. This could be the consequence of a particularly active soil dust present in the local region. n_s for illite-NX ~~is~~ was compared to that of Hiranuma et al. (2015), who combined immersion freezing data from several direct processing INP methods to develop a n_s parameterization. Here, we used the Gumbel cumulative distribution linear fit parameters derived from dry dispersion measurements to generate the n_s fit. ~~The present~~Our data agree within one order at warmer (-28 to -30°C) and colder temperatures (-34 to -38°C), but at other temperatures (-30 to -34°C) the data diverge. Finally, we compared our data with n_s parameterization from Steinke et al. (2016). Steinke et al. (2016) used immersion freezing data from four soil dust samples (Mongolian soil, Karlsruhe soil, German soil, and Argentinian soil) to produce a n_s fit that is valid over a temperature range between -26 to -11°C. We extrapolated the n_s fit toward colder temperatures, and comparison shows higher n_s values but overlaps within the order of magnitude with others.

Figure 7 (a, c, and d) also shows the n_s results reported by five different direct processing INP instruments used in the FIN-02 campaign (DeMott et al., 2018). Our data for K-feldspar nearly align with the others at warmer temperatures (> -28°C). For the illite-NX sample, agreement with the PIMCA-PINC method is within one order of magnitude, but the agreement is observed within two orders of magnitude with others. The present data for Argentinian soil dust aligns with the PIMCA-PINC method and agrees with the others within one order of magnitude. The discrepancy between ~~present~~ our results and others' could be attributed to the different capabilities employed by individual measurement methods to investigate the immersion freezing properties. The experimental uncertainties (e.g. ice crystal detection limit, RH and temperature error limits) from these methods could also influence the n_s results. Previously evaporative freezing by contact nucleation inside-out has been hypothesized to explain the higher freezing temperatures and rates of ice formation observed during droplet evaporation (Durant and Shaw, 2005). Durant and Shaw (2005) showed that water droplets containing individual insoluble INPs freeze at a higher temperature compared to the immersion freezing mechanisms. We cannot rule out that the evaporative freezing mechanism may be occurring in our experiments, and it would be responsible for the higher ns values compared to other studies. The comparison with the CIC-PNNL chamber showed that present data agree within one order of magnitude. Note that CIC-PNNL (PNNL ice chamber but operated in a traditional mode; Friedman et al., 2011; Kulkarni et al., 2012) was operated at RH_w = 106%, and its operation limited investigating immersion freezing on the entire particle population. It can be observed that for illite-NX and Argentinian soil dust samples a correction factor of 4 up to 5 is needed to apply to the CIC-PNNL data to match with the data from the ~~new mode of chamber operation~~MCIC.

Our results can guide design considerations for future CFDC-style ice chambers. The length of conditioning section can be increased so that higher RH_w values would not be necessary to activate all the particles to sufficiently large droplet sizes (≈ 2 µm in diameter). This design feature could help to increase the lifetime of the ice layer. Based on CFD results (Fig. S3-5), the minimum evaporation/nucleation length required is 0.2 m. In addition, implementing a separate refrigeration system to independently cool the nucleation section, the new operation mode presented here can be adapted.

4   Conclusions

32

An alternative method of operating a CFDC-style ice chamber referred as MCIC was explored to ~~detect~~ determine the immersion freezing ability of INPs. This new mode of operation allowed us to obtain maximum immersion freezing fractions of INPs without droplet breakthrough ambiguity. Here, instead of investigating immersion freezing at discrete temperatures, immersion freezing was investigated by activating particles to droplets at high RH_w followed by steady cooling under imposed ice-saturated conditions. The chamber performance was evaluated by testing the ice nucleation ability of four INP materials: K-feldspar, illite-NX, Argentinian soil dust, and airborne arable dust particles. In addition, we performed CFD simulations to evaluate flow, humidity, and temperature performance. The results indicate that these three thermodynamic conditions are locally fully developed, which confirms constant mass and thermal flux, and therefore steady operating conditions within the chamber. Tests using size-selected AS particles showed that homogeneous freezing of solution droplets occurs in agreement with theory and previous study results, and that to activate all the particles to droplets high RH_w values of ~~-~$\approx$113% are needed. Analytical and CFD calculations indicate that such high values are needed to grow the droplets to larger sizes so that they can survive long enough to induce freezing and to allow the particles that may have escaped the aerosol lamina to activate into droplets. Tests using the four INP materials demonstrated the activation of all individual particles to generate immersion freezing spectra in terms of F_{ice} and n_s. Experimental results indicate that K-feldspar minerals induced detectable ice formation at ~~-~$\approx$-22°C and maximum F_{ice} (= 90%) was observed at -28°C. The other three samples induced nucleation of ice at temperatures colder than -26°C, and their maximum F_{ice} (= 90%) was observed to be ~~-~$\approx$-36°C. The F_{ice} was normalized using particle surface area to calculate the n_s, and these n_s calculations show that our results are comparable to the parameterizations and data reported in the literature. We find that the majority of our n_s results are higher within one order of magnitude than others. Analysis of such high temporal resolution immersion freezing measurements could offer better insights into the freezing properties of INPs, thereby moving us toward improved representations of the immersion freezing ability of INPs for cloud models.

Data availability. Data plotted in this paper are available upon request.

Author contribution. GK analyzed the data and wrote the paper. NH, OM, KK, SC, DC and PJD contributed and commented on all results. SC provided airborne arable dust composition and morphology results.

Competing interests. The authors declare that they have no conflict of interest.

1185

References

Ansmann, A., Tesche, M., Seifert, P., Althausen, D., Engelmann, R., Fruntke, J., Wandinger, U., Mattis, I., and Muller, D.: Evolution of the ice phase in tropical altocumulus: SAMUM lidar observations over Cape Verde, *J Geophys Res-Atmos*, 114, Artn D17208 10.1029/2008jd011659, 2009.

ANSYS Fluent 14.0. (2016). ANSYS Inc, Canonsburg, PA, USA.

Atkinson, J. D., Murray, B. J., Woodhouse, M. T., Whale, T. F., Baustian, K. J., Carslaw, K. S., Dobbie, S., O'Sullivan, D., and Malkin, T. L.: The importance of feldspar for ice nucleation by mineral dust in mixed-phase clouds (vol 498, pp 355, 2013), *Nature*, 500, 491-491, 10.1038/nature12384, 2013.

Baron, P. A. and Willeke, K.: Aerosol Measurement: Principles, Techniques, and Applications, 2nd ed., Wiley-Interscience Publications, 2001.

Boose, Y., Kanji, Z. A., Kohn, M., Sierau, B., Zipori, A., Crawford, I., Lloyd, G., Bukowiecki, N., Herrmann, E., Kupiszewski, P., Steinbacher, M., and Lohmann, U.: Ice Nucleating Particle Measurements at 241 K during Winter Months at 3580m MSL in the Swiss Alps, *J Atmos Sci*, 73, 2203-2228, 10.1175/Jas-D-15-0236.1, 2016.

Boucher, O., Randall, D., Artaxo, P., Bretherton, C., Feingold, G., Forster, P., Kerminen, V.-M., Kondo, Y., Liao, H., Lohmann, U.,Rasch, P., Satheesh, S. K., Sherwood, S., Stevens, B., and Zhang, X. Y.: Climate Change 2013 The Physical Science Basis; Working Group I Contribution to the Fifth Assessment Report of the Intergovernmental Panel on Climate Change, Cambridge, United Kingdom and New York, NY, USA, 571-657, 2013.

1190

1195

1200

1205

Broadley, S. L., Murray, B. J., Herbert, R. J., Atkinson, J. D., Dobbie, S., Malkin, T. L., Condliffe, E., and Neve, L.: Immersion mode heterogeneous ice nucleation by an illite rich powder representative of atmospheric mineral dust, *Atmos Chem Phys*, 12, 287-307, 10.5194/acp-12-287-2012, 2012.

1210 Budke, C., and Koop, T.: BINARY: an optical freezing array for assessing temperature and time dependence of heterogeneous ice nucleation, *Atmos Meas Tech*, 8, 689-703, 10.5194/amt-8-689-2015, 2015.

Chen, Y. L., Kreidenweis, S. M., McInnes, L. M., Rogers, D. C., and DeMott, P. J.: Single particle analyses of ice nucleating aerosols in the upper troposphere and lower stratosphere, *Geophysical Research Letters*, 25, 1391-1394, Doi 10.1029/97gl03261, 1998.

1215 Chou, C., Stetzer, O., Weingartner, E., Juranyi, Z., Kanji, Z. A., and Lohmann, U.: Ice nuclei properties within a Saharan dust event at the Jungfraujoch in the Swiss Alps, *Atmos Chem Phys*, 11, 4725-4738, 10.5194/acp-11-4725-2011, 2011.

DeMott, P. J., Prenni, A. J., Liu, X., Kreidenweis, S. M., Petters, M. D., Twohy, C. H., Richardson, M. S., Eidhammer, T., and Rogers, D. C.: Predicting global atmospheric ice nuclei distributions and their impacts on climate, *P Natl Acad Sci USA*, 107, 11217-11222, 10.1073/pnas.0910818107, 2010.

1220 DeMott, P. J., Prenni, A. J., McMeeking, G. R., Sullivan, R. C., Petters, M. D., Tobo, Y., Niemand, M., Mohler, O., Snider, J. R., Wang, Z., and Kreidenweis, S. M.: Integrating laboratory and field data to quantify the immersion freezing ice nucleation activity of mineral dust particles, *Atmos Chem Phys*, 15, 393-409, 10.5194/acp-15-393-2015, 2015.

DeMott, P. J., Mohler, O., Cziczo, D. J., Hiranuma, N., Petters, M. D., Petters, S. S., Belosi, F., Bingemer, H. G., Brooks, S. D., Budke, C., Burkert-Kohn, M., Collier, K. N., Danielczok, A., Eppers, O., Felgitsch, L., Garimella, S., Grothe, H.,
1225 Herenz, P., Hill, T. C. J., Hohler, K., Kanji, Z. A., Kiselev, A., Koop, T., Kristensen, T. B., Kruger, K., Kulkarni, G., Levin, E. J. T., Murray, B. J., Nicosia, A., O'Sullivan, D., Peckhaus, A., Polen, M. J., Price, H. C., Reicher, N., Rothenberg, D. A., Rudich, Y., Santachiara, G., Schiebel, T., Schrod, J., Seifried, T. M., Stratmann, F., Sullivan, R. C., Suski, K. J., Szakall, M., Taylor, H. P., Ullrich, R., Vergara-Temprado, J., Wagner, R., Whale, T. F., Weber, D., Welti, A., Wilson, T. W., Wolf, M. J., and Zenker, J.: The Fifth International Workshop on Ice Nucleation phase 2
1230 (FIN-02): laboratory intercomparison of ice nucleation measurements, *Atmos Meas Tech*, 11, 6231-6257, 10.5194/amt-11-6231-2018, 2018.

Durant, A. J., and Shaw, R. A.: Evaporation freezing by contact nucleation inside-out, *Geophysical Research Letters*, 32, Artn L20814 10.1029/2005gl024175, 2005.

Friedman, B., Kulkarni, G., Beranek, J., Zelenyuk, A., Thornton, J. A., and Cziczo, D. J.: Ice nucleation and droplet formation
1235 by bare and coated soot particles, *J Geophys Res-Atmos*, 116, Artn D17203 10.1029/2011jd015999, 2011.

Garimella, S., Kristensen, T. B., Ignatius, K., Welti, A., Voigtlander, J., Kulkarni, G. R., Sagan, F., Kok, G. L., Dorsey, J., Nichman, L., Rothenberg, D. A., Rosch, M., Kirchgassner, A. C. R., Ladkin, R., Wex, H., Wilson, T. W., Ladino, L. A., Abbatt, J. P. D., Stetzer, O., Lohmann, U., Stratmann, F., and Cziczo, D. J.: The SPectrometer for Ice Nuclei (SPIN): an instrument to investigate ice nucleation, *Atmos Meas Tech*, 9, 2781-2795, 10.5194/amt-9-2781-2016, 2016.

Garimella, S., Rothenberg, D. A., Wolf, M. J., David, R. O., Kanji, Z. A., Wang, C., Rosch, M., and Cziczo, D. J.: Uncertainty in counting ice nucleating particles with continuous flow diffusion chambers, *Atmos Chem Phys*, 17, 10855-10864, 10.5194/acp-17-10855-2017, 2017.

Herbert, R. J., Murray, B. J., Whale, T. F., Dobbie, S. J., and Atkinson, J. D.: Representing time-dependent freezing behaviour in immersion mode ice nucleation, *Atmos Chem Phys*, 14, 8501-8520, 10.5194/acp-14-8501-2014, 2014.

Hiranuma, N., Augustin-Bauditz, S., Bingemer, H., Budke, C., Curtius, J., Danielczok, A., Diehl, K., Dreischmeier, K., Ebert, M., Frank, F., Hoffmann, N., Kandler, K., Kiselev, A., Koop, T., Leisner, T., Mohler, O., Nillius, B., Peckhaus, A., Rose, D., Weinbruch, S., Wex, H., Boose, Y., DeMott, P. J., Hader, J. D., Hill, T. C. J., Kanji, Z. A., Kulkarni, G., Levin, E. J. T., McCluskey, C. S., Murakami, M., Murray, B. J., Niedermeier, D., Petters, M. D., O'Sullivan, D., Saito, A., Schill, G. P., Tajiri, T., Tolbert, M. A., Welti, A., Whale, T. F., Wright, T. P., and Yamashita, K.: A comprehensive laboratory study on the immersion freezing behavior of illite-NX particles: a comparison of 17 ice nucleation measurement techniques, *Atmos Chem Phys*, 15, 2489-2518, 10.5194/acp-15-2489-2015, 2015.

Hoose, C., and Mohler, O.: Heterogeneous ice nucleation on atmospheric aerosols: a review of results from laboratory experiments, *Atmos Chem Phys*, 12, 9817-9854, 10.5194/acp-12-9817-2012, 2012.

Ignatius, K., Kristensen, T. B., Jarvinen, E., Nichman, L., Fuchs, C., Gordon, H., Herenz, P., Hoyle, C. R., Duplissy, J., Garimella, S., Dias, A., Frege, C., Hoppel, N., Troestl, J., Wagner, R., Yan, C., Amorim, A., Baltensperger, U., Curtius, J., Donahue, N. M., Gallagher, M. W., Kirkby, J., Kulmala, M., Mohler, O., Saathoff, H., Schnaiter, M., Tome, A., Virtanen, A., Worsnop, D., and Stratmann, F.: Heterogeneous ice nucleation of viscous secondary organic aerosol produced from ozonolysis of alpha-pinene, *Atmos Chem Phys*, 16, 6495-6509, 10.5194/acp-16-6495-2016, 2016.

Jones, H. M., Flynn, M. J., DeMott, P. J., and Mohler, O.: Manchester Ice Nucleus Counter (MINC) measurements from the 2007 International workshop on Comparing Ice nucleation Measuring Systems (ICIS-2007), *Atmos Chem Phys*, 11, 53-65, 10.5194/acp-11-53-2011, 2011.

Kanji, Z. A., and Abbatt, J. P. D.: The University of Toronto Continuous Flow Diffusion Chamber (UT-CFDC): A Simple Design for Ice Nucleation Studies, *Aerosol Sci Tech*, 43, 730-738, Pii 910471828 10.1080/02786820902889861, 2009.

Kanji, Z. A., Welti, A., Chou, C., Stetzer, O., and Lohmann, U.: Laboratory studies of immersion and deposition mode ice nucleation of ozone aged mineral dust particles, *Atmos Chem Phys*, 13, 9097-9118, 10.5194/acp-13-9097-2013, 2013.

Kanji, Z. A., Ladino, L. A., Wex, H., Boose, Y., Burkert-Kohn, M., Cziczo, D. J., & Krämer, M.: Overview of ice nucleating particles, *Meteorological Monographs*, 58, 1.1-1.33, https://doi.org/10.1175/AMSMONOGRAPHS-D-16-0006.1, 2017.

Knopf, D. A., Alpert, P. A., and Wang, B. B.: The Role of Organic Aerosol in Atmospheric Ice Nucleation: A Review, *Acs Earth Space Chem*, 2, 168-202, 10.1021/acsearthspacechem.7b00120, 2018.

Kohn, M., Lohmann, U., Welti, A., and Kanji, Z. A.: Immersion mode ice nucleation measurements with the new Portable Immersion Mode Cooling chAmber (PIMCA), *J Geophys Res-Atmos*, 121, 4713-4733, 10.1002/2016JD024761, 2016.

Kulkarni, G., Fan, J., Comstock, J. M., Liu, X., and Ovchinnikov, M.: Laboratory measurements and model sensitivity studies of dust deposition ice nucleation, *Atmos Chem Phys*, 12, 7295-7308, 10.5194/acp-12-7295-2012, 2012.

Lohmann, U., and Feichter, J.: Global indirect aerosol effects: a review, *Atmos Chem Phys*, 5, 715-737, DOI 10.5194/acp-5-715-2005, 2005.

Murphy, D. M., and Koop, T.: Review of the vapour pressures of ice and supercooled water for atmospheric applications, *Q J Roy Meteor Soc*, 131, 1539-1565, 10.1256/qj.04.94, 2005.

Murray, B. J., O'Sullivan, D., Atkinson, J. D., and Webb, M. E.: Ice nucleation by particles immersed in supercooled cloud droplets, *Chem Soc Rev*, 41, 6519-6554, 10.1039/c2cs35200a, 2012.

Niedermeier, D., Augustin-Bauditz, S., Hartmann, S., Wex, H., Ignatius, K., and Stratmann, F.: Can we define an asymptotic value for the ice active surface site density for heterogeneous ice nucleation?, *J Geophys Res-Atmos*, 120, 5036-5046, 10.1002/2014jd022814, 2015.

Niemand, M., Mohler, O., Vogel, B., Vogel, H., Hoose, C., Connolly, P., Klein, H., Bingemer, H., DeMott, P., Skrotzki, J., and Leisner, T.: A Particle-Surface-Area-Based Parameterization of Immersion Freezing on Desert Dust Particles, *J Atmos Sci*, 69, 3077-3092, 10.1175/Jas-D-11-0249.1, 2012.

Pruppacher, H. R. and Klett, J. D.: Microphysics of Clouds and Precipitation, Springer Publications, New York, USA, 954 pp., 1997.

Rogers, D. C.: Development of a continuous flow thermal gradient diffusion chamber for ice nucleation studies, *Atmospheric Research*, 22, 149-181, 10.1016/0169-8095(88)90005-1, 1988.

1295 Rogers, R. R. and Yau, M. K.: A Short Course in Cloud Physics, Pergamon Press, New York, USA, pp 99–120, 1989.

Schiebel, T.: Ice Nucleation Activity of Soil Dust Aerosols, Ph. D. Dissertation,, Institute for Meteorology and Climate Research – Atmospheric Aerosol Research (IMK-AAF), 131, 2017.

Seinfeld, J. H. and Pandis, S. N.: *Atmospheric Chemistry and Physics: From Air Pollution to Climate Change*, Wiley, Ch.17, 2016.

1300 Stetzer, O., Baschek, B., Luond, F., and Lohmann, U.: The Zurich Ice Nucleation Chamber (ZINC) - A new instrument to investigate atmospheric ice formation, *Aerosol Sci Tech*, 42, 64-74, 10.1080/02786820701787944, 2008.

Su, Y. Y., Miles, R. E. H., Li, Z. M., Reid, J. P., and Xu, J.: The evaporation kinetics of pure water droplets at varying drying rates and the use of evaporation rates to infer the gas phase relative humidity, *Phys Chem Chem Phys*, 20, 23453-23466, 10.1039/c8cp05250f, 2018.

1305 Ullrich, R., Hoose, C., Mohler, O., Niemand, M., Wagner, R., Hohler, K., Hiranuma, N., Saathoff, H., and Leisner, T.: A New Ice Nucleation Active Site Parameterization for Desert Dust and Soot, *J Atmos Sci*, 74, 699-717, 10.1175/Jas-D-16-0074.1, 2017.

Vali, G.: Interpretation of freezing nucleation experiments: singular and stochastic; sites and surfaces, *Atmos Chem Phys*, 14, 5271-5294, 10.5194/acp-14-5271-2014, 2014.

1310 Vali, G., DeMott, P. J., Mohler, O., and Whale, T. F.: Technical Note: A proposal for ice nucleation terminology, *Atmos Chem Phys*, 15, 10263-10270, 10.5194/acp-15-10263-2015, 2015.

Vali, G.: Revisiting the differential freezing nucleus spectra derived from drop-freezing experiments: methods of calculation, applications, and confidence limits, *Atmos Meas Tech*, 12, 1219-1231, 10.5194/amt-12-1219-2019, 2019.

Westbrook, C. D., and Illingworth, A. J.: The formation of ice in a long-lived supercooled layer cloud, Q *J Roy Meteor Soc*, 1315 139, 2209-2221, 10.1002/qj.2096, 2013.

Zenker, J., Collier, K. N., Xu, G. L., Yang, P., Levin, E. J. T., Suski, K. J., DeMott, P. J., and Brooks, S. D.: Using depolarization to quantify ice nucleating particle concentrations: a new method, *Atmos Meas Tech*, 10, 4639-4657, 10.5194/amt-10-4639-2017, 2017.
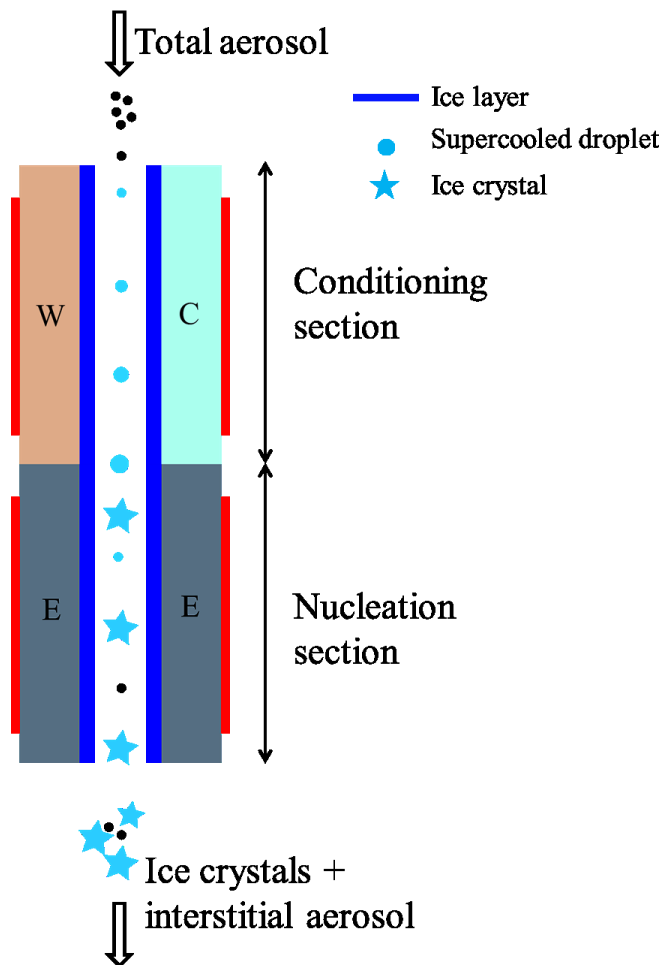
1320

Figure 1: Schematic showing the geometry of the ~~modified ice chamber~~MCIC (expanded for clarity). INP proxies are activated to droplets within the conditioning section, and these supercooled droplets are steadily cooled within the nucleation section, from ~≈-20°C to ~≈-42°C to induce freezing of droplets and evaporate unfrozen supercooling droplets. The residence time in each section of the chamber is ~≈5 s, and the ice layer spans both sections of the chamber. A cyclone impactor upstream of the ice chamber is used to remove the larger particles (>1.5 μm in diameter) while sampling airborne arable dust particles. The heating tapes (red rectangular strip) are attached to the walls to precisely control the temperature of the walls. W –warm wall; C – cold wall; E – Nucleation section wall. The length of both conditioning and nucleation section are 0.45 m. The width of the chamber is 0.15 m. The gap between warm and cold walls is 0.01 m.
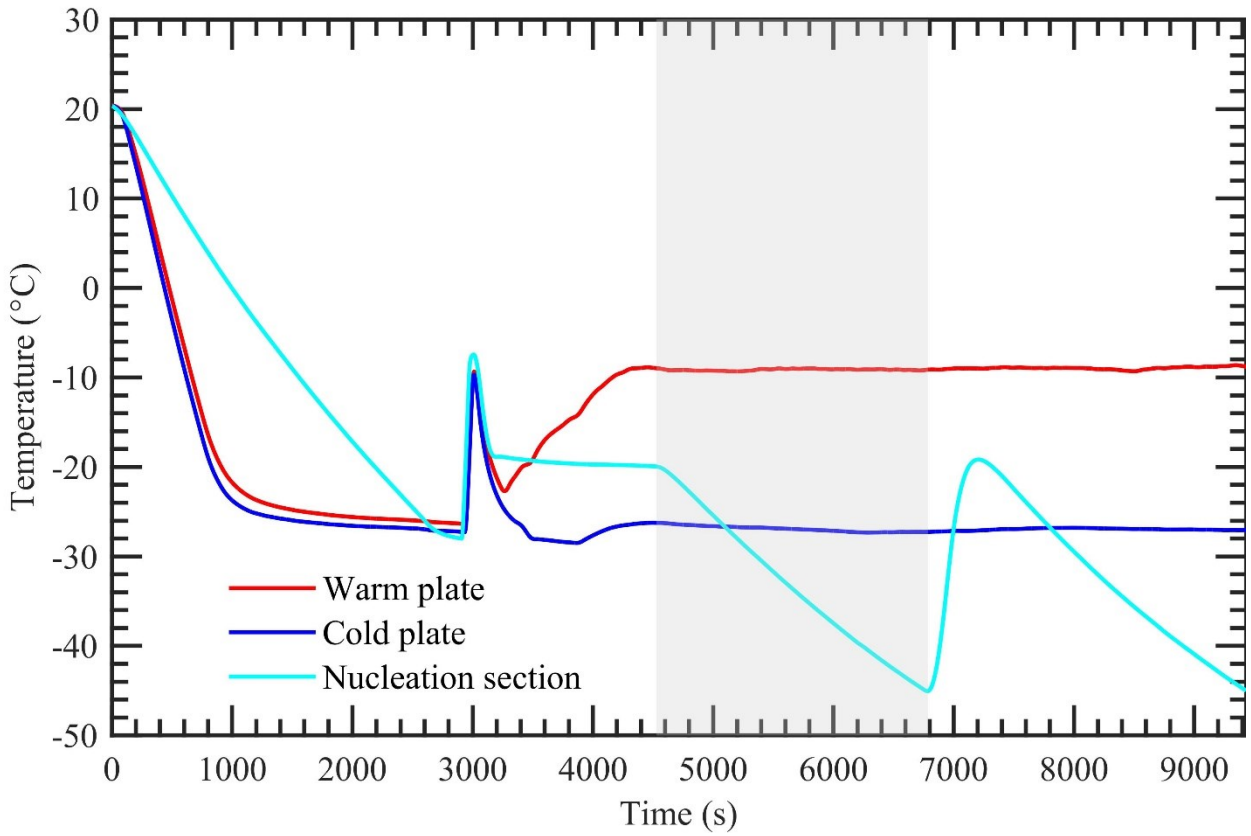
Figure 2: Measured temperature of warm, cold, and nucleation section walls during a typical experiment. The shaded area indicates the experimental conditions during one ice nucleation measurement. During this INP measurement, the temperature of both warm and cold walls is kept constant, while the nucleation section is cooled at a steady rate (0.5°C min⁻¹).

1340
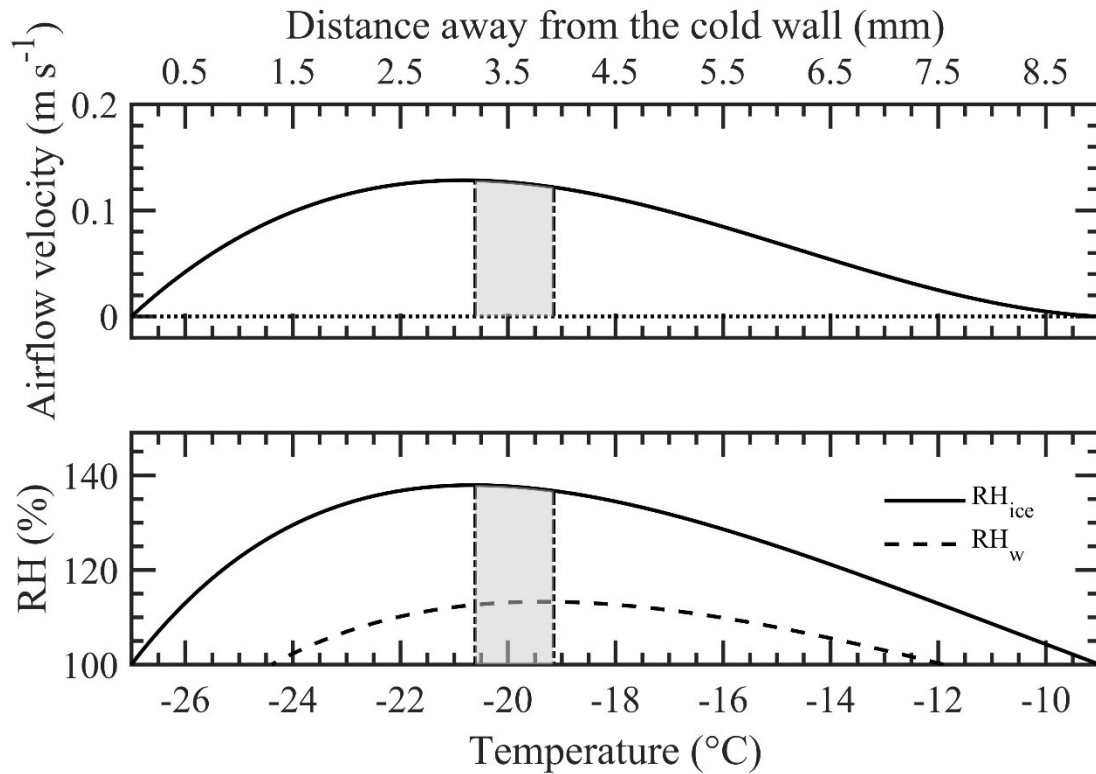
Figure 3: Steady-state airflow velocity and relative humidity (RH) conditions calculated using the mathematical model developed by Rogers (1988) within the conditioning section of the ice chamber. The chamber warm wall (left) and the cold wall (right) are at -9 and -27°C, respectively. The shaded area between the two vertical dashed-dotted lines shows the boundaries of aerosol lamina under at these above temperatures and flow conditions (sheath flow: 5 LPM and sample flow: 1 LPM). The profiles are asymmetric because of the thermophoretic drift of the flow, caused by the thermal gradient between the walls, towards the colder wall. The conditioning section is always supersaturated with respect to ice (RH_{ice}>100%), and except the near-wall positions, the section is also supersaturated with respect to water (RH_w>100%).

1365

1370

1375

Velocity (m/s) RH_{ice} Temperature (°C)
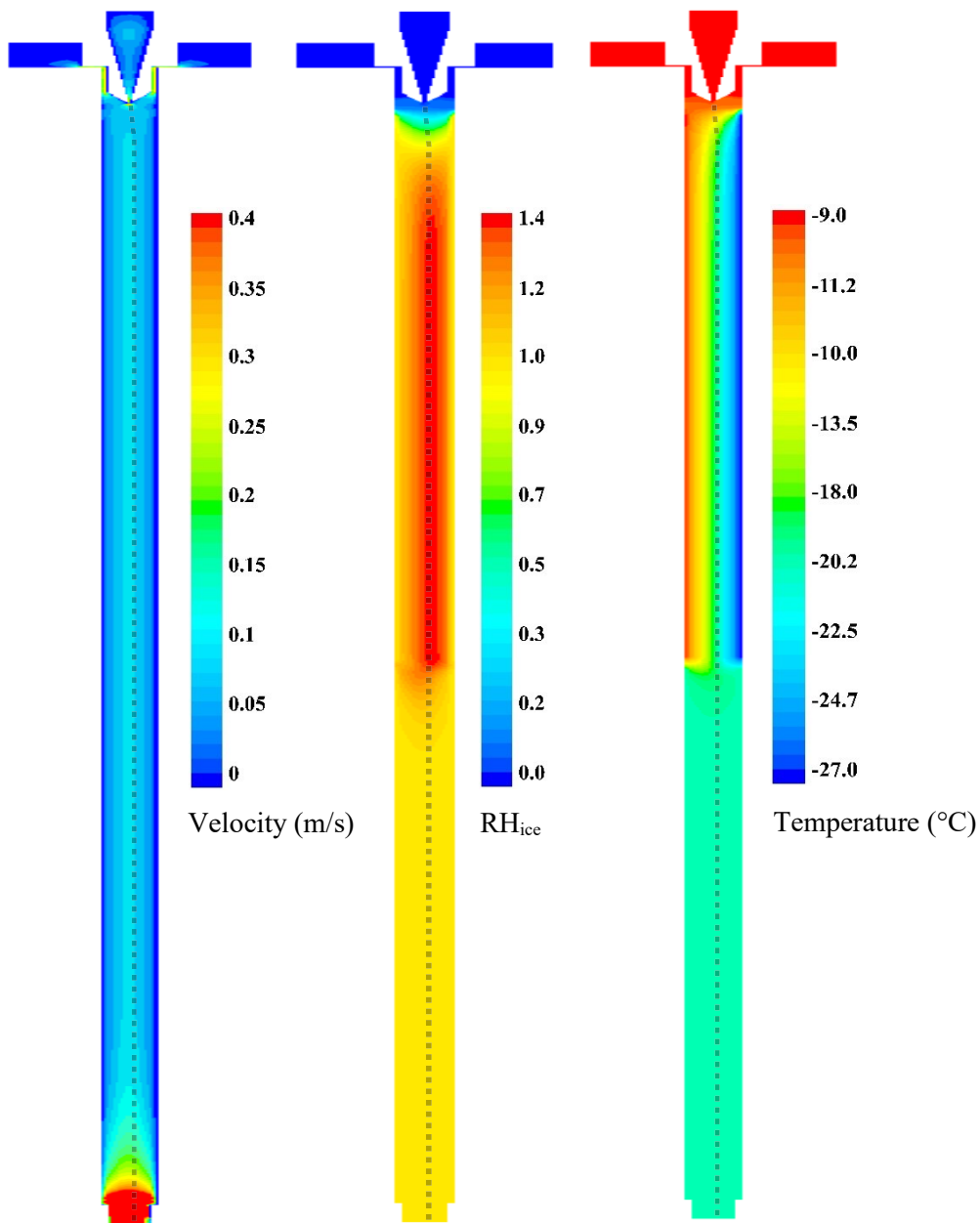
(b)
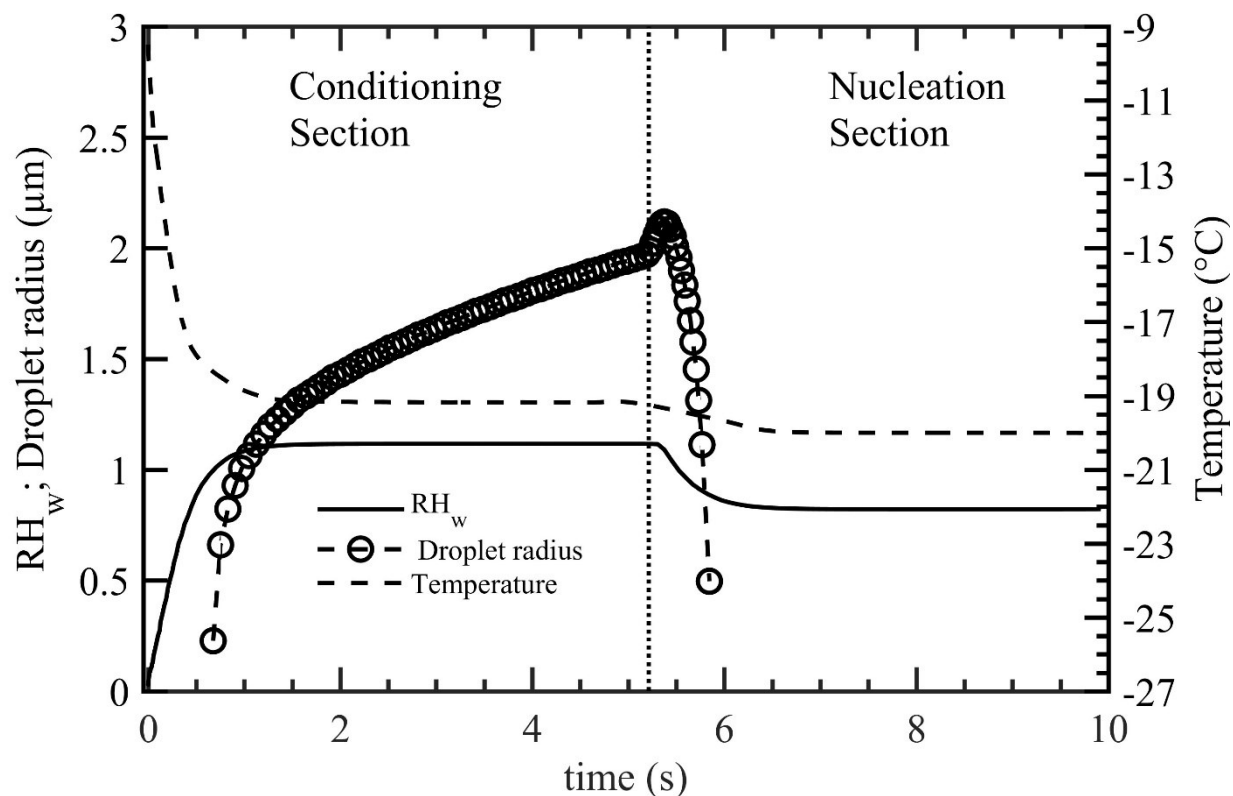
Figure 4: (a) Contours of CFD calculated airflow velocity, RH_{ice}, and temperature profiles within the ice chamber. Warm and cold walls of conditioning section are maintained at -9 and -27°C, respectively. The nucleation section is maintained at -20°C. The dashed line shows the trajectory of a single INP within the aerosol lamina transiting through the chamber. (b) CFD calculated temperature and RH_w profiles of a potential INP released from the sample injection region to the outlet end of the chamber. Analytical calculations of droplet growth and evaporation of such a potential INP (0.3 µm in diameter) are also shown. The left and right sides of the vertical dotted line represent the conditioning and nucleation sections, respectively. See the text for more details. Simulations results at other nucleation section temperatures are shown in Fig. S1-4.
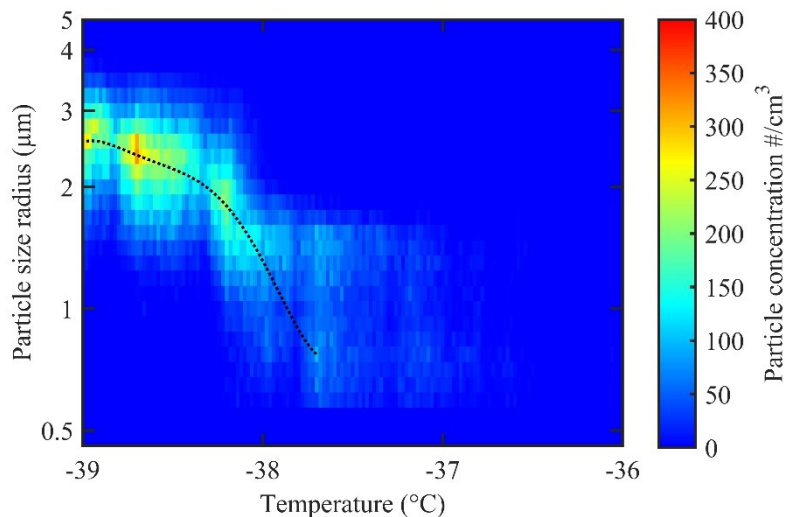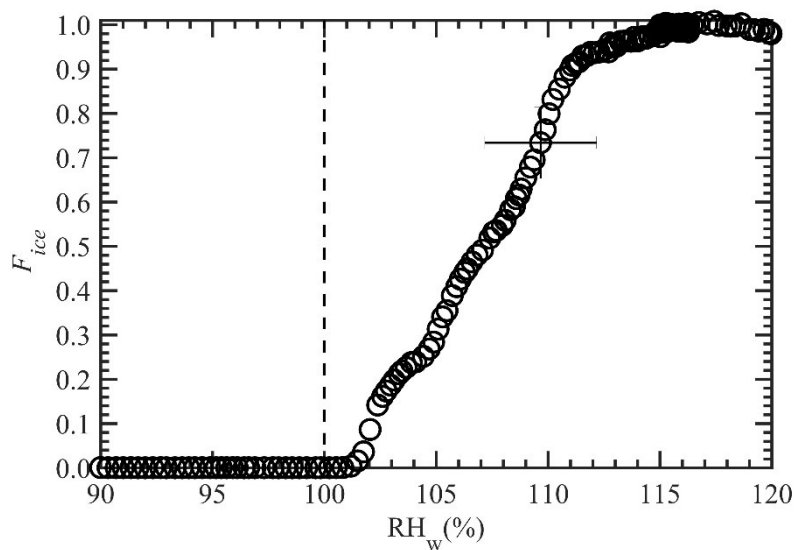
43

(a)

(b)

1395

Figure 5: Homogenous freezing of water droplets containing one wt. % ammonium sulfate solution. (a) OPC classified ice particle concentrations as a function of ice crystal diameter at different temperatures. Warm and cold walls of conditioning section are maintained at -9 and -27°C, respectively. (b) The fraction of frozen solution droplets with RH_w, where the temperature of the nucleation section is maintained constant at -42°C to induce droplet freezing via the homogeneous freezing mode and RH_w within

1400 **the conditioning section was steadily increased from 90 to 120%. Slightly colder temperature (-42°C) than homogeneous freezing limit ($\approx$-38.5°C; panel a) is used to account for the uncertainty within temperature and RH_w conditions. The dashed line in panel (a) and (b) indicate the increase in freezing fraction of droplets trend (for illustration purpose) and the onset of saturation line, respectively. The uncertainty in RH_w is shown as an error bar (see the text for more details). The uncertainty in F_{ice} is one standard deviation (n = 3). For clarity, error bars are shown only for one data point.**
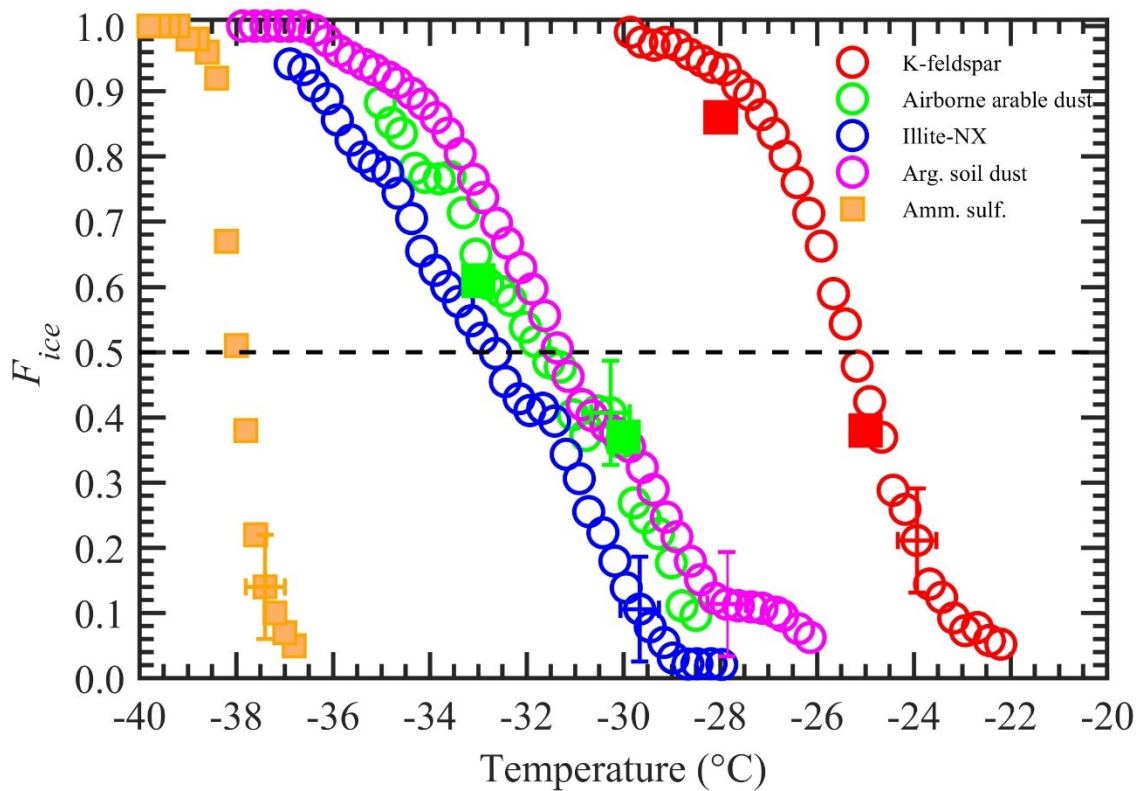
1405

Figure 6: The F_{ice} of four INP test species as a function of temperature. The vertical error bar represents the one standard deviation of the three repeat experiments (n = 3). Temperature measurements had ±0.4°C uncertainty. For clarity, error bars are shown for only one data point. Orange solid square markers represent the freezing temperatures of water droplets containing one wt. % AS. **Other solid square markers represent data collected when the chamber was operated in a steady-state temperature mode (instead**
1410   **of steady cooling).** **The horizontal dashed line represents 50% F_{ice}.**
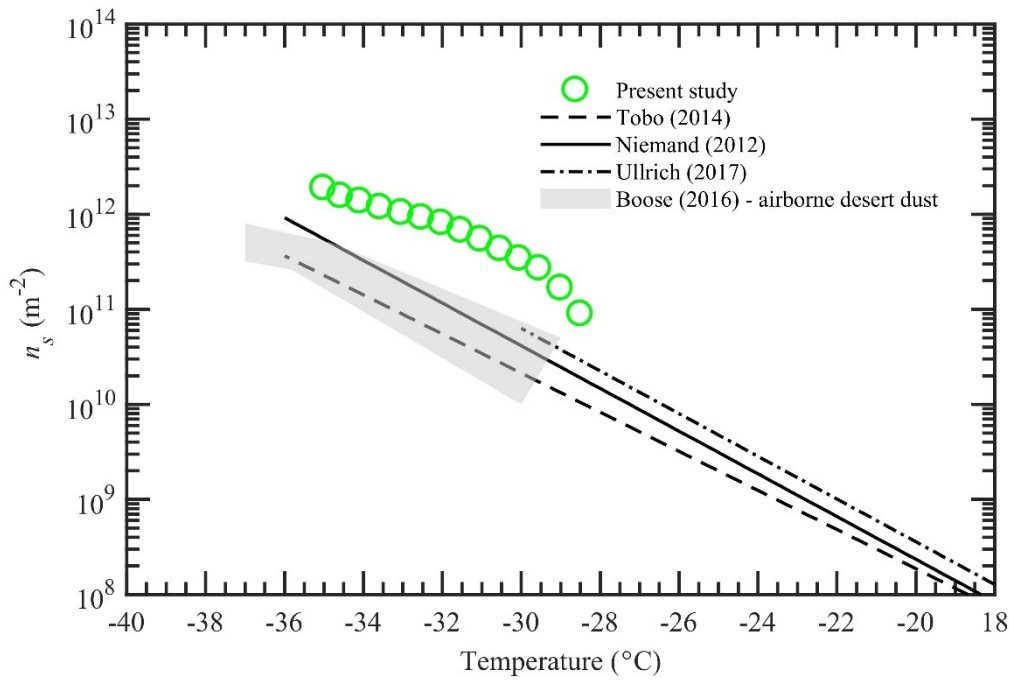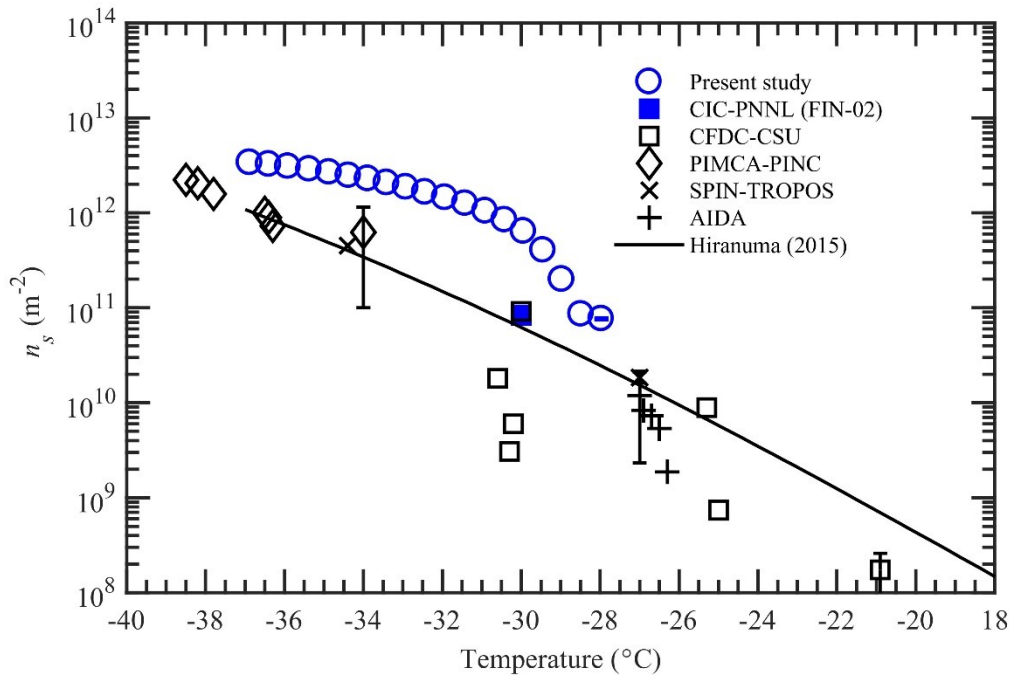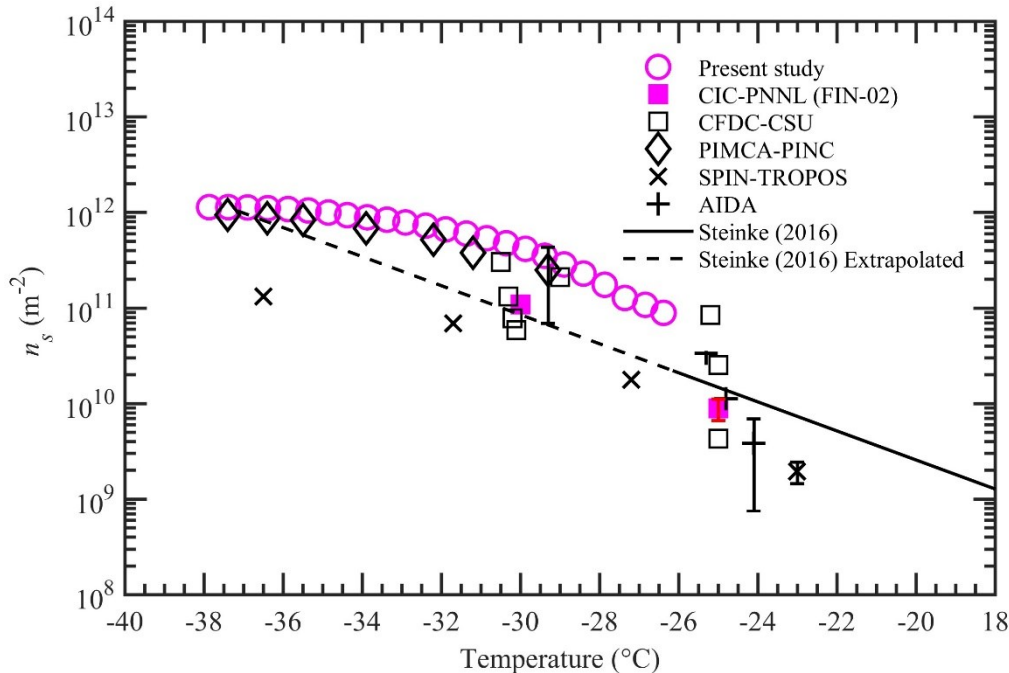
1415
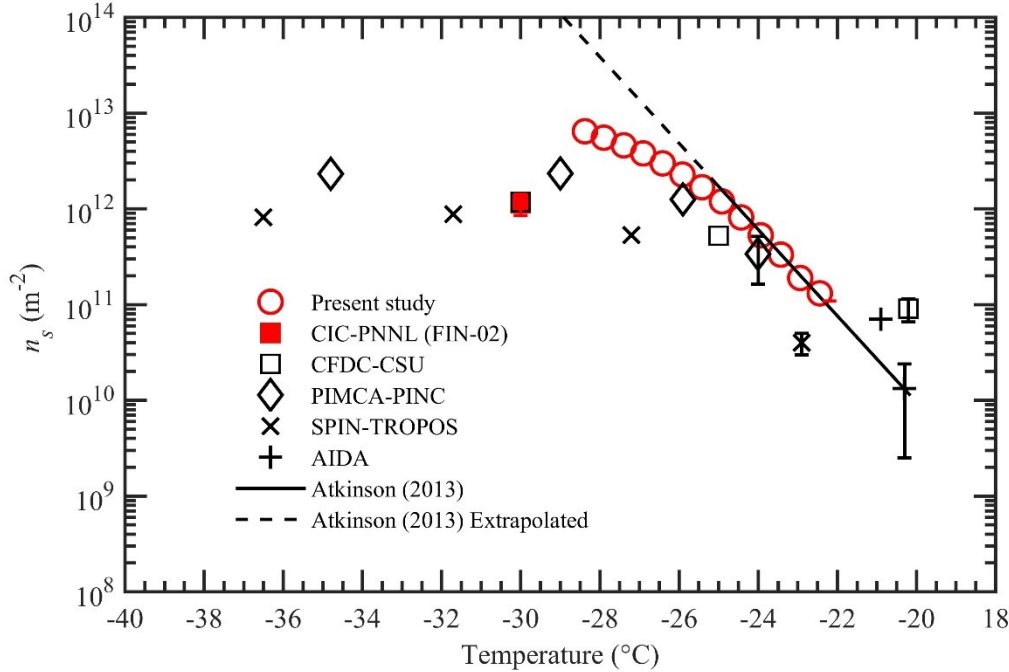
Figure 7: Ice nucleation active site density (n_s) as a function of temperature for four INP test species tested in this study. The panels a) to d) show n_s densities for K-feldspar, airborne arable dust, illite-NX, and Argentinian soil dust, respectively. Solid and dash-dot lines represent various parameterizations from the literature. See the text for details. Dashed lines in panel a) and d) indicate the extrapolated data calculated outside the temperature limits recommended in these n_s parameterizations. The black color symbols

represent n_s values from various other instruments that participated in FIN-02 activity (DeMott et al., 2018). Filled color symbols show the data from the CIC-PNNL chamber but operated at steady-state temperature and RH_w = 106% conditions at FIN-02. For clarity, confidence intervals are shown only for one data point from each study.

1435